NATIONAL ADVISORY COMMITTEE
FOR AERONAUTICS

TECHNICAL NOTE 2171

INVESTIGATION OF A TWO-STEP NOZZLE IN THE

LANGLEY 11-INCH HYPERSONIC TUNNEL

By Charles H. McLellan, Thomas W. Williams,
and Mitchel H. Bertram

Langley Aeronautical Laboratory
Langley Air Force Base, Va.

NACA

Washington

September 1950

1

NATIONAL ADVISORY COMMITTEE FOR AERONAUTICS

TECHNICAL NOTE 2171

INVESTIGATION OF A TWO-STEP NOZZLE IN THE

LANGLEY 11-INCH HYPERSONIC TUNNEL

By Charles H. McLellan, Thomas W. Williams,
and Mitchel H. Bertram

SUMMARY

Flow surveys have been made in the first of several nozzles to be investigated in the Langley 11-inch hypersonic tunnel. The nozzle was designed by the method of characteristics for a Mach number of 6.98. Two 2-dimensional steps were used: the first step expanded the air in the horizontal plane to a Mach number of 4.36 and the second in the vertical plane to a Mach number of 6.98.

The test results showed that, although a maximum Mach number of about 6.5 was obtained, the flow in the test section was not sufficiently uniform for quantitative wind-tunnel test purposes. Deviations from the design flow were traced to the presence of a thick boundary layer which developed in the first step along the parallel walls.

INTRODUCTION

Wind-tunnel equipment capable of producing Mach numbers in excess of 5 is needed to provide basic aerodynamic data in the hypersonic speed range. Above a Mach number of approximately 4, however, the difficulties of obtaining acceptable flow in a wind tunnel increase rapidly with Mach number. Among the factors involved are the large area expansion ratios, the large variations in static pressure from the settling chamber to the test section, the large temperature reduction that takes place through the nozzle, and the large pressure ratios required to maintain the flow.

A project was undertaken involving the construction of a pilot hypersonic wind tunnel in which the flow problems could be studied. An intermittent type of tunnel was chosen which discharged air from a

high-pressure tank with an initial pressure of about 50 atmospheres through the nozzle and test section into a vacuum tank. This type of tunnel was selected so that very high pressure ratios could be provided across the system. A test section 10 inches square was selected as approximately the smallest practical size from the consideration of accuracy of construction, test-model dimensions, and flow-survey details. Operation of the hypersonic tunnel was begun November 26, 1947. The first of a series of nozzles investigated in this tunnel was the two-step or double-expansion $M = 6.98$ nozzle discussed in this paper. Included in the series of nozzles is a single-step nozzle, designed for $M = 7.0$, which is currently under investigation. The scope of the present paper is limited to the investigation of the flow through the two-step nozzle.

<div align="center">SYMBOLS</div>

M Mach number

p_w wall static pressure

p_0 settling-chamber pressure

p_0' stagnation pressure after a normal shock

p_s cone-surface static pressure

T_0 settling-chamber temperature, $^\circ F$ absolute

T_0' stagnation temperature, $^\circ F$ absolute

δ apparent boundary-layer thickness

ϵ_h flow angle in horizontal plane

ϵ_v flow angle in vertical plane

γ ratio of specific heats ($\gamma = 1.40$)

θ shock angle

X longitudinal station measured from throat (table I)

Y lateral station measured from vertical center line (table I)

Z vertical station measured from horizontal center line (table I)

THE PROBLEMS OF THE HYPERSONIC TUNNEL

As mentioned previously, this investigation was undertaken to study the problems to be met in designing hypersonic tunnels. The most important of these problems result from the following factors:

(1) The large area ratios

(2) The large pressure ratios across the system required to maintain the flow

(3) The large decrease in free-stream temperature that takes place through the nozzle

(4) The large variations in static pressure through the nozzle

The large area expansion from the first minimum, or $M = 1$ section, to the test section, or final Mach number section (104.1:1 at $M = 7$), creates many difficulties. In general, it means that the first minimum area becomes very small and requires extremely accurate machine work. The flow in the nozzle is also very sensitive to small boundary-layer changes at the first minimum. For the approximately 10-inch-square test section of the nozzle used in this investigation, the first minimum area is about 1 square inch. In a conventional two-dimensional nozzle, this would amount to a slit 1/10 inch high and 10 inches wide, whereas at a Mach number of 10 this slit would be reduced to a height of about 0.020 inch. Nozzles which avoid the need for a thin slitlike first minimum are the two-step nozzle which may have an almost square throat and the three-dimensional nozzle. The three-dimensional form of nozzle involves many design problems, particularly if optical viewing of the flow is required.

Also encountered at the high Mach numbers is the difficulty of providing the large pressure ratios required to drive the tunnel. For example, the stagnation-pressure ratio across a normal shock at $M = 7$ is about 65, while at $M = 10$ it becomes about 328. Use of these shock losses as a rough index to the required pressure ratios indicates that, with reasonable size and densities, large amounts of power will be required to drive a hypersonic tunnel. Of course, by the use of second minimums (that is, an area reduction after the test section) a substantial reduction in the pressure ratio required to maintain flow can be expected.

A third major obstacle to overcome in order to obtain a satisfactory flow is the heating requirement. In order to maintain the static temperature of the air above the liquefaction temperature in the test section, the stagnation temperature must be increased to a point at

which many structural problems are encountered and the design of heaters is extremely difficult. Thus, with a 50-atmosphere stagnation pressure at $M = 7$, a stagnation temperature of about 640° F is required to maintain the air above the liquefaction point. At $M = 10$, this temperature increases to approximately 1400° F. The liquefaction temperature of air was assumed to be that of oxygen at its partial pressure. Slightly higher temperatures than these are preferable because of the difficulties of evaluating the ratio of the specific heats near the liquefaction point and the intereffect of the components of the air on the liquefaction point.

The wide range of pressures experienced in the nozzle gives rise to some difficulties. Thus, the methods of measurement must be changed from those used in normal wind-tunnel practice. For example, the optical means of observing the flow must be extremely sensitive because of the extremely low densities encountered in the test section, even with reasonably high stagnation pressures. The pressures in the test section are low even with stagnation pressures of the order of 50 atmospheres. These low pressures make the accurate measurement of pressures difficult. High stagnation pressures are also required if the realm of aerodynamics in which the mean free path of the gas molecules becomes appreciable is to be avoided.

Over the wide range of pressures and temperatures encountered in hypersonic wind tunnels, some deviation from the perfect-gas laws can be expected. These effects are somewhat minimized by using a high stagnation temperature with the high stagnation pressure. For a Mach number 7 tunnel with stagnation pressures up to 50 atmospheres and a stagnation temperature around 1000° F absolute, the imperfect-gas effects can be neglected.

Several of these foregoing factors tend to have a large but difficult-to-analyze effect on the boundary layer found in the nozzle. High stagnation temperatures and heat conduction through the boundary layer tend to cause large viscosity gradients. In the portions of the nozzle in which large static-pressure gradients occur, there is a large stabilizing effect on the boundary layer tending to keep it laminar and thin. The Reynolds number is also of importance inasmuch as a high Reynolds number has a destabilizing effect on the laminar boundary layer.

APPARATUS

General description.— The hypersonic tunnel of this investigation, which was designed primarily to operate over a range of Mach numbers from 6 to 10, is shown schematically in figure 1. The high pressure

ratio required to overcome shock and boundary-layer losses is supplied·
by discharging air from a high-pressure tank to a vacuum tank. These
tanks are shown in figures 2 and 3. The high-pressure tank stores
400 cubic feet of 50-atmosphere air which is emitted through a motorized
$2\frac{1}{2}$-inch valve to a heat exchanger where the air is heated. From the
heat exchanger, the air passes through a quick-opening valve to the
settling chamber, then through the nozzle, and by way of a 24-inch valve
to the cooler, and into the 12,000-cubic-foot vacuum tank. The portion
of the tunnel from the heat exchanger to the 24-inch valve is shown in
figure 4.

The tunnel, although of the intermittent type, has a closed system
wherein the air in the vacuum tank is pumped back into the high-pressure
tank by means of a vacuum pump and a three-stage compressor connected in
series. Reuse of test air by means of the closed system reduces the
drying problem. As shown in the diagrammatic arrangement (fig. 1), the
two pumps are driven simultaneously from a common drive. After leaving
the last stage of the compressor, the air passes through an oil and
moisture trap and an air filter before being dried and discharged to
the high-pressure tank. The drying is accomplished at the pressure of
50 atmospheres at which it is possible to remove approximately all but
1 part of water in 2,000,000 parts of air. This high degree of dryness,
however, was seldom obtained in practice. The air in the dryer is
maintained at the high pressure by a regulating valve on the discharge
side.

The heat exchanger is of the heat-storage type and is shown in
cutaway in figure 5. It consists of a cast alloy steel case packed with
copper tubing. The tubing is arranged in four groups to reduce the rate
of heat conduction from the downstream end to the upstream extremity
which is cooled most during the running period; thus the temperature
of the air leaving the heater is maintained essentially constant. The
heat exchanger is brought up to temperature over a long period of time
by heating elements wrapped around the case.

This heater has several disadvantages, the most objectionable being
a copper-oxide scale which forms on the copper tubing with the result
that particles of scale are swept downstream during the period of
running. Most of this scale was being carried into the nozzle with the
initial blast of air as the quick-opening valve was opened. Much of the
copper oxide could be eliminated from the stream by using the much more
slowly opening motorized valve upstream of the heat exchanger to start
the run. Heating the heat exchanger while evacuated or while filled
with an inert gas such as nitrogen in order to retard the rate of
scaling was also advantageous.

Another difficulty encountered with the heat exchanger is the poor heat conduction from the heaters to the innermost tubes. This factor requires a lengthy heating period and effectively limits the maximum temperature of the air out of the heater to about 850° F.

In order to avoid having a high Mach number stream with a high stagnation pressure entering the large tube downstream of the nozzle and possibly damaging the turning vanes and cooler during the first few seconds of running time when extremely high pressure ratios are available, a choke or reduced-area section was placed in the passageway ahead of a 24-inch valve. The choke was of such a size that supersonic flow could not be established in the 2-foot pipe upstream of the choke so that a shock loss and a reduced total pressure occurred upstream of the coolers and vanes.

A cooler was placed before the vacuum tank in order to cool the hot air and thus increase the effectiveness of the vacuum tank.

An additional vacuum pump capable of obtaining very high vacuums was also provided in order to reduce the vacuum-tank and tunnel pressure sufficiently to allow tests to be made with stagnation pressures as low as 1 atmosphere.

Nozzle.- The nozzle surveyed is of the double-expansion type. In this form of nozzle, the first minimum is more nearly square than that in the single-step two-dimensional nozzle. The first step expands the gas two-dimensionally to a Mach number intermediate between unity and the final Mach number. In the second step, the gas expands at right angles to that in the first expansion to the final Mach number. The nozzle tested is shown in figure 6 with the top plate of the first expansion and one of the side plates of the second expansion removed to show the nozzle contours. Another view is shown in figure 7 which includes a test-section side plate with a schlieren viewing window in place. The nozzle is shown in place in the tunnel in figure 8.

The method of characteristics was used to design both steps of the nozzle. The throat is 1.500 inches high by 0.667 inch wide, thus the first minimum area is 1 square inch. The first nozzle was designed to expand air from the throat to a section 1.500 inches high by 9.950 inches wide with a Mach number of 4.36. The second expansion commences with a sudden break of 10.25° in the 9.950-inch-wide wall and expands the air to a final design Mach number of 6.98. The test-section dimensions with this nozzle are 9.950 inches in width by 10.514 inches in height.

The nozzle design ordinates are presented in table I. These are the theoretical ordinates based on the method of characteristics with no allowance for boundary layer.

INSTRUMENTATION

The large range of conditions through the nozzle associated with the high Mach number and the short time of operation available have required considerable change in techniques and procedures of surveying the flow from those commonly used.

Pressure recording.— Wall pressures, for example, vary from 46 atmospheres in the settling chamber to about 10 millimeters of mercury or less in the test section. The pressures and operating conditions at these extremes make conventional manometers impractical. Furthermore, the short duration of the run requires that a short time lag and a time history of the pressures be obtained. (The settling-chamber pressure, for example, may vary during a run from 46 atmospheres at the start of the run to 34 atmospheres at the end.)

The pressure—recording instruments shown in figures 9 and 10 were developed for this project by the Instrument Research Division of the Langley Aeronautical Laboratory and are an adaptation of a type used in flight. The bellows of the low—pressure cells is of the nesting type so that it can be exposed to atmospheric pressure without damage. The internally evacuated bellows expands when the external pressure is reduced; this expansion is converted into a rotation of a small mirror which reflects a beam of light to a moving film, thereby giving a time history of the pressure. An accuracy of about one-half of 1 percent of full—scale deflection can be obtained through careful calibration and reading of the records of the extremely low pressure measuring cells. The accuracy is of the same order for the cells in the range up to 2 atmospheres; however, since the full—scale deflections of these cells are not usually obtained during tests, an average accuracy of about 1 percent is obtained for individual test points. For the instrument cells used in the measurement of pressures in the ranges above 2 atmospheres, an accuracy of 1 percent at full—scale deflection is obtained. The instruments are insensitive to room temperature over the range normally encountered in testing.

Schlieren system.— The schlieren system used is of the double—traverse coincident type as shown in figure 11. The system was so constructed that either horizontal or vertical viewing through the test section, vertical viewing through the first expansion, and horizontal viewing through the second expansion could be obtained. The double—traverse coincident type of schlieren system was used because of the high degree of sensitivity such a system affords. A large radius of curvature (20 ft) on the 12—inch—diameter spherical mirror was also used to obtain a high sensitivity. Although the path of light rays through the section being viewed is conical, the deviation from parallel is negligible in most cases because of the large radius of curvature and

the small effective aperture of this mirror. The system has been found to be extremely sensitive; in fact, it is limited primarily by the quality of the windows which were the best available at the time. A schlieren photograph of the windows is shown in figure 12(a). An indication of the schlieren sensitivity can be obtained from figure 12(b), which is a schlieren photograph of the flow about a 4° included-angle cone at a Mach number of 6.5. At this Mach number, the theoretical density change across a shock on the cone is only about 1.3 percent of the free-stream density which is about 6 to 7 percent of atmospheric density. These shock patterns from the 4° cone were too close to the limiting sensitivity for consistently good schlieren photographs to be obtained; therefore, the majority of the tests were made using a 10° included-angle cone, and a few tests were made with a 5° cone. A schlieren photograph of the flow about the 10° cone used in the survey is shown in figure 13, along with a photograph with no flow showing the window flaws and reference lines. The density increase across the shock from the 10° cone is theoretically about 18 times as great as that for the 4° cone. The schlieren photographs were obtained with the use of a mercury vapor lamp and an exposure of 1/50 of a second.

METHODS AND PROCEDURES

Wall pressures.— Static wall pressures along the nozzle were obtained from 0.025-inch-diameter orifices in the side wall plates. These pressures were used in conjunction with the settling-chamber pressure or the total pressures to determine Mach numbers.

Cone pressures.— Pressures were obtained from orifices installed on the survey cones. For example, on the 10°-included-angle cone, orifices were located 90° apart as shown in figure 14.

The ratio of the average cone surface pressure to the value of the stagnation pressure after the normal shock p_0' from the pressure-recovery survey at each station was used to obtain the Mach number. The method of computing the flow about cones from references 1, 2, 3, and 4 combined with the normal-shock equations was used to determine the Mach number and flow angles. This method assumes uniform irrotational flow.

Schlieren survey.— Mach numbers and flow angles have been determined from schlieren photographs of the shocks from cones. With uniform flow, the Mach number and flow angle may be obtained from the shock angles by using the theoretical studies of the flow about cones parallel to the flow and cones at small angles of yaw of references 1 and 2 and the tabulated values in references 3 and 4. In this present investigation, however, the flow is nonuniform with large variations in both flow angle and Mach number.

For the purpose of obtaining approximate measurements of the flow
in the present investigation, the shock angle at any point is assumed to
be a unique function of the cone angle, the Mach number, and the flow
angle immediately ahead of the shock at the point under consideration.
This assumption is exact only when the strength of the shock is reduced
to zero. With the relatively weak shock from the cones tested, however,
this assumption is believed to give reasonably good accuracy.

Because it is impossible to make a cone with a perfect point and to
maintain a fine point for a series of tests, and because the effects of
boundary—layer growth are the greatest at the point of the cone, the
shock angles were not measured at the vertex. Instead, the shock angles
were measured at two arbitrary stations located approximately 2
and 4 inches from the vertex of the cone. The shock angles were plotted
against position (Y-axis on diagram) with the use of the station on the
shock as the point under investigation. In the following diagram
θ_a is plotted against Y_a and θ_b against Y_b. Thus, in this fashion,
two curves are obtained, one for the lower shock from the cone and the
other for the upper shock. From the faired curves of these plots is
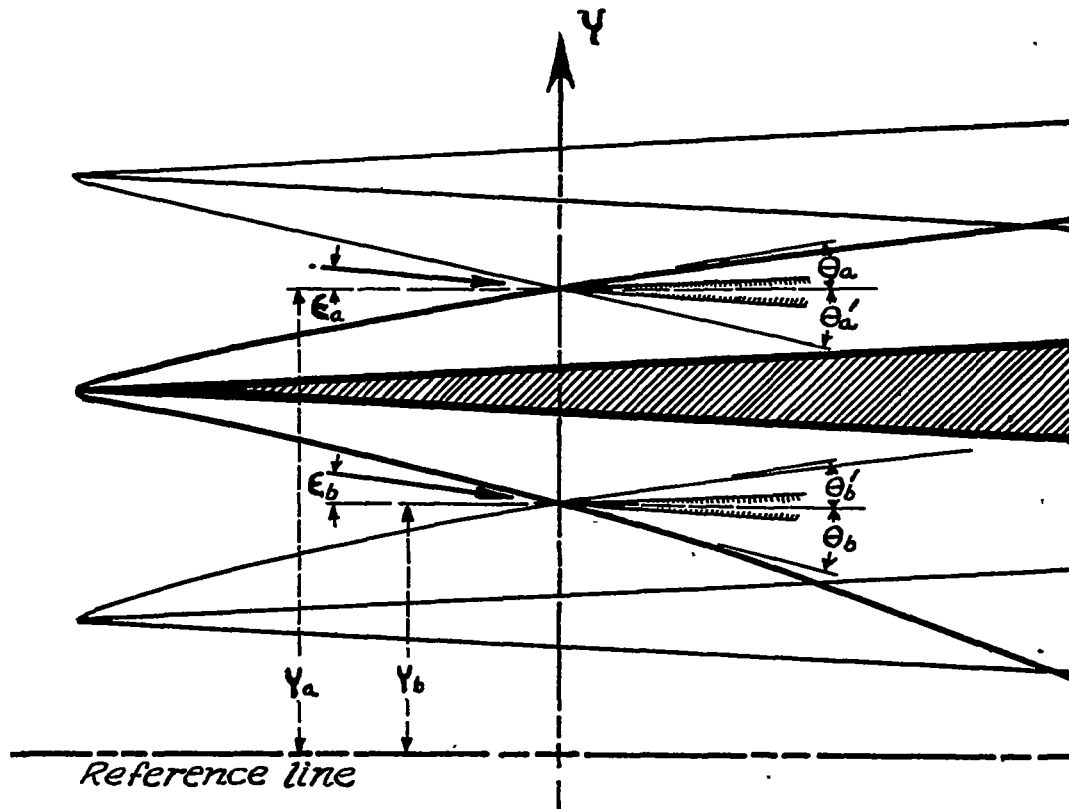
obtained the value of the upper and lower shock angles at the station.
The average of these angles is used to determine the Mach number.

As shown in the figure, this procedure is assumed to give the same
results as if a perfect cone with the same angle as the test cone were
placed at the stations being investigated (Y_a and Y_b on diagram) and
the shocks from its vertex measured.

The flow angle at a station can be expressed as a function of the
difference in the shock angles and the Mach number, which has been
determined. For example, at any point Y being investigated for a
given cone angle

$$\epsilon = \frac{\Delta\theta}{f(M)}$$

Thus, by means of the tables of reference 3, the flow angle is determined
in the viewing plane of the schlieren system.

Disturbance patterns.— Disturbance patterns in the first expansion
were obtained by the use of the schlieren system. Thin tapes about
0.0035 inch thick and 1/4 and 1/2 inch wide were used on the nozzle
blocks to provide the disturbance. Because, in the first expansion, the
air is not expanded sufficiently to drop the static temperature below
the liquefaction point with the air unheated and no noticeable change in
wall static pressure occurred with changes in stagnation temperature,
the patterns in the first nozzle were obtained with the stagnation
temperature approximately equal to room temperature. Because of the
high stagnation temperature required to avoid liquefaction and a thick
boundary layer, satisfactory patterns were not obtained for the second
expansion.

Total—pressure survey.— The stagnation-pressure probes used in the
nozzles are shown in figure 14. In the first expansion, a small probe
projected from the tunnel wall and extended to the center of the stream.
The round tube from which the pressure tubes project was shown to have
no effect on the pressure readings inasmuch as the pressures were
independent of the length of the measuring tubes. The pressure
measured by these tubes is the pressure behind the normal shock which
forms across the front of the tube. At the end of the first nozzle,
this pressure is approximately one—tenth of the stagnation pressure. In
the test section at the design Mach number, the total—head tubes read
only 1.5 percent of the free—stream total pressure.

The static pressures have been obtained from wall orifices and have been assumed constant laterally across the test section (that is, no variation with the Y coordinate) at the given XZ-station.

Stagnation temperature.— The stagnation–temperature survey was made with the temperature probe shown in figure 14. This probe is a light-weight double-shielded thermocouple with bleed holes at the rear of the shields which allow a small amount of air to flow through the probe. The probe was designed to be as light as possible so as to give a minimum of temperature lag. The ratio of the temperatures of the probe and the settling-chamber thermocouple reached a steady value over the latter part of the run.

Free-stream static pressures.— No free-stream static pressures were obtained because the poor flow in the nozzles made their measurement difficult. Since the nozzle appeared unsatisfactory for testing purposes, further or more complete surveys than herein described were not warranted.

Operating conditions.— Plots of the results of a typical test run are presented in figure 15. Although the stagnation pressure varies appreciably during the test period, the ratio of the wall static pressure to settling-chamber pressure remains essentially constant. In this figure, the duration of the run is seen to be approximately 30 seconds, with conditions reasonably well stabilized after 8 seconds. In general, the settling-chamber temperature is maintained between 650° and 850° F. Slightly lower temperatures were obtained for the special tests at low settling-chamber pressures because of the high-percentage heat losses at the low pressures. All runs, however, were made with the test-section static temperature above the liquefaction temperature for the pressures at which the tests were made.

The dew point of the air in the system was maintained at a temperature below -50° F at atmospheric pressure for all runs.

In the nozzle, the free-stream Reynolds number per foot of length is high because of high air velocities and the low viscosity, even though the density is low. In the constant Mach number section at the end of the first expansion, a Reynolds number of about 14×10^6 per foot is obtained which decreases to about 4.8×10^6 per foot at the test section. (The test-section Reynolds number per foot is that which would be experienced at an altitude of about 60,000 ft at a Mach number of 7.)

RESULTS AND DISCUSSION

Wall-pressure surveys.— Pressure measurements were made along the
center line of the parallel walls of the first nozzle. The pressures
have been converted to indicated Mach numbers ($\gamma = 1.4$ isentropic flow)
which are presented in figure 16 along with a theoretical or design Mach
number distribution. Through the first portion of the nozzle, the
theoretical and experimental curves are nearly identical. As the constant
Mach number portion of the curve is approached, the experimental curve
drops below the theoretical. This deviation is attributed largely to
the growth of boundary layer and is discussed in more detail in a later
section.

The variation of the theoretical and experimental indicated Mach
number distribution along the center line of the wall of the second
expansion is presented in figure 17. This figure indicates that the
actual expansion starts earlier than the theoretical expansion and that
appreciable effect from boundary layer occurs at the sudden expansion.
The nozzle is not functioning as the design conditions predicted. A
maximum indicated Mach number along the center line of 6.67 is obtained
at station 66. Beyond this station, a wavy distribution is obtained
which probably originates from the poor flow at the start of the second
expansion.

The pressures were measured over most of the flat wall of the first
expansion. These results are presented in figure 18 as a Mach number
contour plot. The top half of the figure presents the theoretical or
design contours, whereas the lower half shows the experimental contours.
Small crosses in this figure show the location of the pressure orifices
from which the results were obtained. The pressures in the first
portion of this expansion agree reasonably well with the theoretical
pressures until a Mach number of about 4.10 is obtained. Beyond this
point, the actual contours differ greatly from the theoretical. As
shown previously in figure 16, the final design Mach number is never
reached. The variation in indicated Mach number over the center and
rear portion of first expansion of the nozzle is actually small and
represents a maximum variation of little over 1 percent.

A similar contour plot is presented in figure 19 for the second
expansion. The difference shown between the theoretical and experimental
contours indicates that a completely different type of flow is taking
place from that for which the nozzle was designed. The deviation of the
contours from the theoretical is too great to be explained by any
simple system of expansion and compression waves. It is interesting to
note that a maximum indicated Mach number of 6.79 was obtained at the
66-inch station slightly off the center line. A small area about
8 inches long and 3 inches high in the test section had less than

a 1-percent variation in Mach number. These Mach numbers obtained from wall pressures and settling-chamber pressure are subject to unknown corrections due to losses in total pressure and variations in static pressure from the wall to the center of the stream.

Disturbance patterns in first expansion.- Schlieren photographs, shown in figures 20(a) and 20(b), were taken of the disturbance pattern caused by the tape. The exposure time for figure 20(a) was a few microseconds, while that for 20(b) was 1/50 second. Also, in figure 20(b), some of the upstream tape has been removed. Figure 20(c) is a schlieren picture without flow which shows the flaws in the windows and reference wires.

From these and other similar schlieren photographs, the comparison shown in figure 21 has been made between the shock patterns and theoretical Mach waves. In general, the disturbance from the front edge of the tape indicates slightly higher shock angles than the theoretical Mach angle; however, the disturbance from the rear of the tape at a point 2 inches downstream of the first minimum has the same angle as a Mach wave. The strength of a shock from the leading edge of a 0.0035-inch-thick tape apparently cannot be entirely neglected in determining the Mach angle in the flow. This comparison shows that no strong disturbances exist in this part of the expansion, which is indicated also by the wall-pressure survey.

During the study of the disturbance in the first expansion, a photograph was obtained of the breakdown of the supersonic flow as the shock progressed upstream. This photograph is presented as figure 22 for general interest. The upstream end of the turbulent area does not appear to be the shock front but probably results from boundary-layer separation caused by the high pressures behind the shock traveling upstream ahead of the shock through the boundary layer. Shocks can be seen to travel into the turbulent area.

Total-pressure survey in the first expansion.- The results from a total-pressure survey can be used to indicate losses in the stream, for with constant static pressure, the lower the pressure recovery, the lower the total pressure. Care must be exercised, however, when a corresponding static-pressure survey is not obtained since a lower pressure recovery could also indicate a higher Mach number if the total pressure is constant and the static pressure variable. In the case under consideration where the distance between the walls is small, a loss in recovery primarily indicates a loss in total pressure. The pressure recovery at the end of the first nozzle is shown in figure 23. At the center line (that is, at $Y = 0$), there is essentially no region of constant pressure recovery; thus this plot indicates that nearly all the flow is boundary layer in this region. Out from the center line (that is, at $Y = -2.25$ and $Y = -4.00$), the recovery pressure does

not fall off so rapidly toward the wall. Figure 24, which is a contour plot of the recoveries across the end of the first step, also shows these results. This figure again indicates that the growth of the boundary layer is the greatest at the center line. An examination of the apparent boundary layer estimated from total-pressure recoveries along the longitudinal center line of the first expansion is shown in figure 25. Indicated by this figure is a very rapid rate of growth and resulting very thick boundary layer in the last 80 percent of the nozzle along the center line. The high Reynolds number in this portion of the nozzle and the absence of any primary stabilizing effects indicate that the boundary layer should be turbulent. The figure shows that the boundary layer in the turbulent form seems to begin approximately 4 inches after the throat. The boundary layer before this point is too thin to be measured by the method used. Thus, a laminar boundary layer is indicated from stations 0 to 4 which can be explained by the presence of a very favorable pressure gradient in this region which tends to have a large stabilizing influence though the Reynolds number is high. The thicker region of low-energy air at the center (see fig. 24) can be explained on the basis that the air here travels in a region of essentially constant pressure for a greater length of surface than the air flowing on either side, as can be seen in figure 18. The boundary layer at the center line is thickened also by the flow of boundary layer from the relatively high pressure region near the nozzle blocks toward the center line of the wall.

Total-pressure survey in the second expansion.- The pressure recoveries measured by total-head tubes across the test section are shown in figure 26. At the vertical center line, the total pressure drops away very rapidly toward the walls. At 2 inches each side of the vertical center line, the pressure recovery first increases, then decreases toward the wall. A more complete survey of the pressure recovery in the test section is shown in figure 27 as a contour plot. This figure shows a large low-pressure area protruding into the stream from the top and bottom. It is shown subsequently that there is a general flow in toward the center of the stream. Along the horizontal center line, a low-pressure-recovery area also projects into the stream, which probably results from the same type of boundary-layer flow which was encountered in the first step. Pressure-recovery factors could not be obtained closer to the side walls with the strut used because of choking of the flow between the wall and the strut.

Temperature recovery.- Figure 28 presents the results from a temperature survey made by a stagnation-temperature probe. The contours in this figure are ratios of absolute stagnation temperature to absolute settling-chamber temperature. This figure shows that a large area of low-energy air is projecting into the stream just as was shown in figure 27. The lower stagnation-temperature recoveries represent considerable loss in total energy in these parts of the stream.

Recovery factors of over 98.5 percent should not be expected since stagnation probes with negligible heat losses are difficult to construct.

Effect of settling-chamber pressure on pressure recovery and indicated Mach number.— In surveys of this nozzle, large changes in settling-chamber pressure were found to have an appreciable effect upon the indicated Mach number. This effect is shown in figure 29 for one station at the end of the second expansion and three stations in the test section. These plots indicate that a decrease in the settling-chamber pressure has only a slight tendency to diminish the Mach number at the high pressures; the diminution of Mach number increases as the settling-chamber pressure is decreased to moderate values, and, at small pressures, the Mach number decreases rapidly with decreasing pressure.

The primary changes that give rise to this effect occur in the boundary layer of the first expansion and affect the entire nozzle flow. This is indicated by the changes shown in the pressure recovery taken at the end of the first expansion for various settling-chamber pressures in figure 30. This figure shows that the deviation between the curves for the highest settling-chamber pressure and the curves for the lower pressures increases as the pressure decreases. The deviation is small between 45 and 22 atmospheres and comparatively large between 22 and 10 atmospheres and below. The variation in Mach number is also affected by changes in heat conduction in the flow as the settling-chamber pressure is lowered. Thus, figures 29 and 30 indicate that the effect of changing boundary layer on indicated Mach number assumes a large magnitude below about 15 atmospheres.

It is interesting to note that the lowest stagnation pressures obtained in this survey correspond to test-section stream pressures of about 1 millimeter of mercury. At this pressure with the low free-stream temperature existing in the test section, the mean free path of the free-stream air is approximately 0.001 inch, while in the boundary layer the mean free path is increased to roughly 0.005 inch and the free path may begin to have a slight effect on the boundary layer.

Test-section Mach number.— The Mach numbers in the test section are presented in figures 31 to 33 as calculated from:

(1) Wall and settling-chamber pressure

(2) Wall and total-head tube pressures

(3) Cone surface pressures and total-head tube pressures

(4) A schlieren cone shock survey

The Mach number across the test section, calculated from wall pressures and settling-chamber stagnation pressure (with isentropic flow assumed), is compared in figure 31 with the Mach number distribution at three stations across the test section calculated from the wall static and total-head tube pressures. Both methods assume that no static-pressure gradients exist across the width of the test section, and the vertical static-pressure distribution at the wall was assumed to apply at all stations across the width of the stream. At the center of the test section (Z = 0), the results of the two methods differ by about 7 percent. At Y = 0, this difference increases extremely rapidly as the wall is approached, the Mach number from the total-head and wall pressures dropping off to comparatively low values; at Y = 2 and -2, this same drop occurs but starts a greater distance out from the vertical center line. Figure 26 shows that the total-head-tube readings are extremely low at the horizontal walls. These low readings explain the large drop in the Mach number toward these walls as obtained from the total-pressure readings. The difference in the Mach number between the two methods can be explained largely on the basis that the flow in the nozzle is not isentropic and that large losses occur. A small part of this dissimilarity can also be caused by the fact that the wall static pressures probably do not accurately indicate the free-stream static pressure, and the value of γ (the ratio of the specific heats) may not be in exact accord with the assumption of $\gamma = 1.40$.

Although the pressure recovery was measured at station X = 89.7 and the static pressures at X = 90.5 in the test section, the error caused by the difference in the actual static pressures and pressure recoveries between the two stations may be neglected because of their closeness.

The results of four surveys of Mach number have been included in figure 32 for the vertical center line and 2 inches to either side at station 90.5. These surveys are:

(1) Mach number from wall static pressure and pressure recovery (replotted from fig. 31)

(2) Mach number from cone surface pressure and pressure recovery

(3) Mach number from measurement of shock angles from a 10° cone

(4) Mach number from measurement of shock angles from a 4° cone

At the vertical center line, the Mach numbers calculated from the wall static and total-head-tube readings agree with the results from the 10°-cone surface pressures. The values obtained from the measurement of shock angles from the 4° cone are somewhat higher than those from the

wall static pressures of the cone surface pressures. Still higher Mach numbers are obtained at the center from the shock angles for the 10°-included-angle cone.

A factor that may partially explain the difference in the curves is the fact that with such a poor distribution the flow is somewhat erratic, and the methods used in making the calculations may not be accurate with such large gradients as are present.

All these plots show that the Mach number decreases greatly toward the top and bottom of the test section; this sharp decrease indicates that at the vertical center line ($Y = 0$), the boundary layer extends to the center of the stream. On each side of the vertical center line (at $Y = 2$ and -2), somewhat flatter distributions are obtained, but again the Mach number drops off greatly, though the drop is displaced to a position nearer the wall and better agreement is obtained between the pressure and shock data. Unfortunately, data for not all the methods were obtained at these positions.

From the comparison of the Mach numbers from the data of wall pressures and the data of cone surface pressures (fig. 32(b)), the percentage static-pressure variation in the stream is seen to be small compared with the percentage variation in total pressure. The Mach number variations are due almost entirely to total-pressure variations.

Figure 33 presents the results for horizontal surveys at three vertical stations at $X = 90.5$. At $Y = 0$ for this station, the Mach number, as determined from cone surface pressures, shows appreciable decreases toward the vertical walls, whereas 2 inches above and below this position the Mach number increases greatly toward the vertical walls. This difference is a consequence of the low-energy region that extends into the flow and has been shown previously; however, appreciable scatter exists. At $Z = 0$, the agreement, between the two methods (cone surface pressure and cone shocks) is good near the center of the stream. Away from the center at $Z = 0$, the cone pressures indicate a decreasing Mach number whereas the results from the measurements of shocks show an increasing Mach number. In this case at $Z = 0$, the results from the cone surface pressures seem to be the more likely.

The Mach number obtained from cone static pressures and total-pressure readings is considered to give the most accurate indication of Mach number in this survey. The Mach number calculated from wall static pressures and the total pressure in the stream agrees with the Mach number determined from the cone static pressures and total-pressure measurement in the stream. In this nozzle, the percentage lateral-static-pressure variation is small compared with the percentage total-pressure variations. The method by which the Mach number is obtained from cone-shock measurements is, in general, subject to inaccuracies

since, for one Mach number range obtained in the test section, the
change in shock angle with large changes in Mach number is small. For
a variation in Mach number from 6.5 to 7.5, the change in shock
semiangle for a 10° cone is only 1°. Probably the best accuracy that
could be expected in measuring cone shocks would be 0.1°. Where the
shock is curved, relatively large errors in determining shock angles
could be expected. Boundary layer on the cone is believed to have had
only a small effect upon the data obtained in the cone surveys. Wall
static and settling-chamber pressures do not accurately determine the
Mach number.

Flow angles in the test section.— Flow angles have been computed
both from the shock angles from cones and from cone surface pressures
and are presented in figures 34 and 35.

The most complete survey of flow angle was obtained at station 88.5
for the vertical flow deflection along the vertical center line
(fig. 34(a)). This figure indicates that at this station there is a
strong vertical flow toward the center of the stream. (Actually the
theory of reference 2, upon which the flow angles were calculated,
assumes that the flow angles are small and that the flow is uniform.)
Considerable stagnation pressure and Mach number gradients are present
in these tests, and, where the flow angles approach 6°, they cannot be
considered small; however, the magnitude of the flow angles is
considered to be approximately correct. This agreement of results
over most of the range between the shock-angle and the cone-surface-
pressure data is considered good.

The horizontal survey of the horizontal flow deflection at $Z = 0$
presented in figure 34(b) indicates that the horizontal flow angles are
small and largely within the accuracy of the measurements.

At station 90.5 at the vertical center line (fig. 35(b)), the flow
angles in the vertical plane are essentially the same as those at
station 88.5 over a large portion of the curve, although less data are
available. One additional curve is included which was taken from 4° cone
data. Reasonable agreement is evident between the methods.

At 2 inches to either side of the vertical center line (figs. 35(a)
and 35(c)), the results from the shock indicate a considerably smaller
flow toward the horizontal center line (actually they indicate flow to
a point slightly above the horizontal center line). A maximum angle of
less than 2° was measured at these stations; however, only shock data
were obtained.

Horizontal flow angles across the test section are presented in
figures 35(d), 35(e), and 35(f). Any definite trends in flow direction

are difficult to determine from these figures, but the angles are comparatively small and, for the most part, within the errors of the measurement technique.

Both methods by which the flow angles in the stream were obtained are subject to large possible errors. The method using cone static pressure depends on a small difference between two pressures. This difference was of the same magnitude as the accuracy of the measurements for low angles. The method using cone–shock angles depends on the measurement of shocks from schlieren photographs. The inaccuracies involved in measuring shock angles have previously been discussed. Both methods are based on the assumption of uniform flow over the area affecting the measurements and on the assumption that the flow angles are small. The flow, however, has been shown to have large gradients, and the flow angles are large. For these reasons, the results from the flow–angle surveys are considered to be qualitative only.

Pressure ratio required to maintain flow.— Because of the poor flow obtained in this nozzle, no specific effort was made to determine the effect of various second–minimum–to–test–section–area ratios upon the pressure ratio required to maintain flow. During the course of the investigation, however, data were obtained for the pressure ratio required with and without the model support strut in place and are presented herewith for general interest. For applications to any but the nozzle reviewed in this report, the data are to be considered merely qualitative.

Without the model support strut, because of a small contraction after the test section, there is a slight second–minimum effect for which the area ratio is 0.951. For this condition, the pressure ratio required was about 150. With the model support strut in place, the area ratio was reduced to 0.779, and the pressure ratio required reduced to approximately 90. Thus, a decrease of 40 percent in the pressure ratio required to maintain flow is obtained. The model support strut, vertically spanning the tunnel just after the test section, was diamond shape in cross section, 2 inches wide and 20 inches long.

General discussion of the nozzle characteristics.— The results have shown that the flow through this nozzle was entirely unsatisfactory for use in a wind tunnel. The origin of the poor flow is in the first expansion of the nozzle. The flow has been shown to follow the theoretical flow to approximately the point at which the center–line Mach number is theoretically constant. Total–pressure studies have shown that just ahead of this point, on the center line of the walls, a rapid growth of apparent boundary layer begins. Furthermore, at the end of the nozzle, the apparent boundary layer is much thicker along the vertical center line than on either side.

The rate of growth of boundary layer along the center line of the side wall of the first expansion is considerably larger than can be accounted for by the compressible turbulent-boundary-layer theories of reference 5. Heat transfer to the walls and boundary-layer flows make an analysis of the boundary layer with the actual nozzle conditions extremely difficult. Throughout most of the length of the nozzle, the pressure at the center line of the parallel walls is much lower than that at the edges near the nozzle blocks. This pressure gradient has a tendency to cause boundary-layer flow from the nozzle blocks toward the center line of the parallel walls. As the flows from the two sides meet at the center line, their momentum carries them into the stream and starts a circulation in the flow. This circulation is apparently carried over into the second nozzle, since a flow toward the center of the stream was found to exist along the vertical center line as far downstream as the test section. The carry-over of this circulation is further evidenced by the region of low-energy air which projects into the stream along the top and bottom of the vertical center line as measured by both total-head tubes and stagnation-temperature thermo-couples. This circulation may be augmented somewhat at the sudden expansion by the poor velocity distribution at the end of the first nozzle. A small countercirculation is apparently set up along the vertical walls of the second expansion as shown by the low-energy areas projecting into each side of the stream along the horizontal center line (fig. 24). The pressure gradients on the side walls of the second expansion would tend to originate the same type of flow in the boundary layer as exists in the first expansion; however, the boundary-layer flow has not so long to develop and also the cross section of the second expansion is of considerably better proportions.

The distance between the parallel walls in the first expansion is so small compared with the distance between the nozzle blocks that this type of boundary-layer flow can have a very pronounced effect on the nozzle flow. The effect of this boundary layer would probably be less if the sudden expansion at the beginning of the second step of the nozzle were replaced by a more gradual one; however, the main cause for the poor flow would still exist. Because the flow is very unfavorable and is virtually all boundary layer at the center line at the end of the first expansion, the present nozzle would be difficult to modify to obtain satisfactory performance. Probably, the most likely method of correcting the flow in this nozzle would be to remove this boundary layer in the first expansion as it builds up, thereby eliminating the possibility of boundary-layer flow and its resulting circulation. The possibility that boundary-layer removal would result in an improvement of the flow in this nozzle can only be conjectural as too large a percentage of the air may have to be removed in order to make the effects of the boundary layer on the flow negligible.

Another possibility of improving the nozzle flow would be to improve the proportions of the first expansion so that the distance between the parallel walls is a greater percentage of the distance between the nozzle blocks. Even with improved proportions boundary-layer removal at the end of the first nozzle would probably be required to obtain satisfactory flow in the second nozzle.

The problems associated with the single-step nozzle appear to be less difficult than those required to make the flow in the two-step nozzle satisfactory. The use of a single-step nozzle therefore appears to be a better approach to obtain satisfactory flow at M = 7. During preparation of this report, tests of a single-step nozzle were in progress. Preliminary inspection of the results indicate that the flow in this design is reasonably uniform both as regards Mach number distribution and stream angularity.

CONCLUDING REMARKS

Tests in an 11-inch hypersonic tunnel have shown that, although a maximum Mach number of about 6.5 was obtained, the two-step or double-expansion nozzle investigated was unsatisfactory for a hypersonic tunnel. Large low-energy areas projected into the stream along the vertical center line of the nozzle. The air flowed toward the center of the stream at large angles on the order of 6° along the vertical center line. A circulation emanating from the flow of boundary layer in the first expansion of the nozzle, combined with the thick boundary layer at the end of the first expansion, appeared to be the cause of the poor flow in the test section. The percentage variations in test-section static pressure were comparatively small as evidenced by the agreement of Mach number from the data of wall pressures and the data of the cone surface pressures. The Mach number variation is almost entirely due to losses in total pressure through the stream.

Settling-chamber pressures had a definite influence upon the nozzle Mach number. The effect was appreciable at settling-chamber pressures below about 15 atmospheres and was traced to changes in the boundary layer of the first expansion with changes in settling-chamber pressure, the variation being appreciable when the settling-chamber pressure was reduced from about 20 to 10 atmospheres.

From the difficulties encountered with this nozzle, it appears that both boundary-layer control and better proportions in the first expansion would be required to obtain satisfactory flow in this type of nozzle.

Preliminary inspection of the results from a single-step nozzle under investigation during the preparation of this report indicates that the flow is reasonably uniform both as regards Mach number distribution and stream angularity.

Langley Aeronautical Laboratory
    National Advisory Committee for Aeronautics
        Langley Air Force Base, Va., August 31, 1949

REFERENCES

1. Taylor, G. I., and Maccoll, J. W.: The Air Pressure on a Cone
      Moving at High Speeds. Proc. Roy. Soc. (London), ser. A, vol. 139,
      no. 838, Feb. 1, 1933, pp. 278-311.

2. Stone, A. H.: On Supersonic Flow Past a Slightly Yawing Cone. Jour.
      Math. and Phys., vol. XXVII, no. 1, April 1948, pp. 67-81.

3. Staff of the Computing Section, Center of Analysis (Under Direction
      of Zdeněk Kopal): Tables of Supersonic Flow around Cones. Tech.
      Rep. No. 1, M.I.T., 1947.

4. Staff of the Computing Section, Center of Analysis (Under Direction
      of Zdeněk Kopal): Tables of Supersonic Flow around Yawing Cones.
      Tech. Rep. No. 3, M.I.T., 1947.

5. Tetervin, Neal: Approximate Formulas for the Computation of Turbulent
      Boundary-Layer Momentum Thicknesses in Compressible Flows. NACA
      ACR L6A22, 1946.

TABLE I

NOZZLE COORDINATES
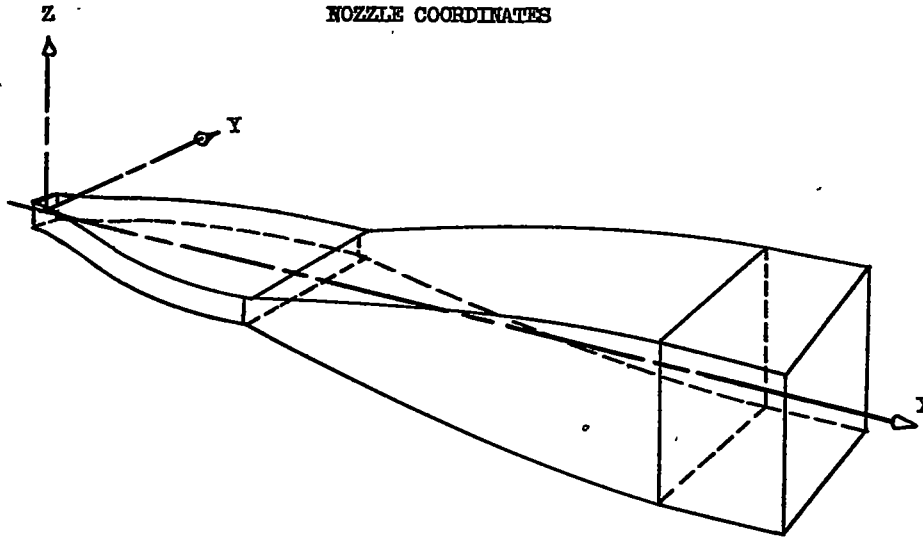
First expansion		Second expansion	
X (in.)	Y (in.)	X (in.)	Z (in.)
0	0.333	31.140	0.750 ⎤ Straight
.100	.335	41.746	2.668 ⎦ line
.200	.341	43.415	2.954
.300	.350	45.311	3.245
.400	.362	47.533	3.546
.500	.378	50.143	3.853
.600	.398	53.218	4.160
.700	.421	56.853	4.459
.800	.448	61.164	4.739
.900	.478	66.292	4.981
1.000	.512	72.416	5.163
1.100	.550	78.003	5.245
1.200	.593	81.484	5.257
1.300	.640	82.015	5.257
1.375	.678		
1.498	.746		
1.866	.938		
2.343	1.172		
2.895	1.415		
3.655	1.721		
4.545	2.043		
5.534	2.362		
6.669	2.683		
8.106	3.038		
9.941	3.425		
12.168	3.815		
14.768	4.178		
17.961	4.506		
22.055	4.783		
26.378	4.939		
30.440	4.975		
31.000	4.975		
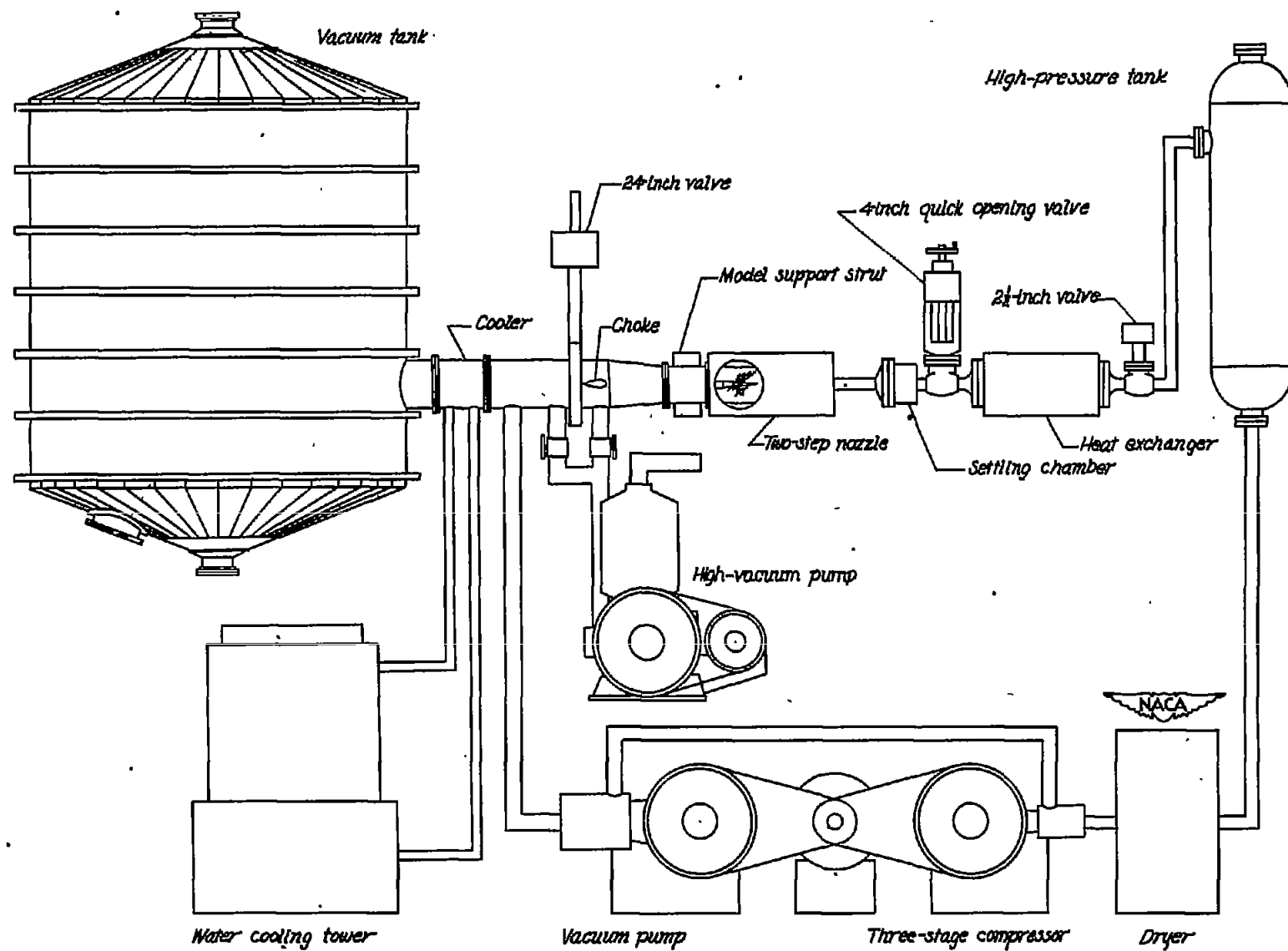
Figure 1.— Schematic diagram of the hypersonic tunnel.

Figure 2.— High-pressure tank..
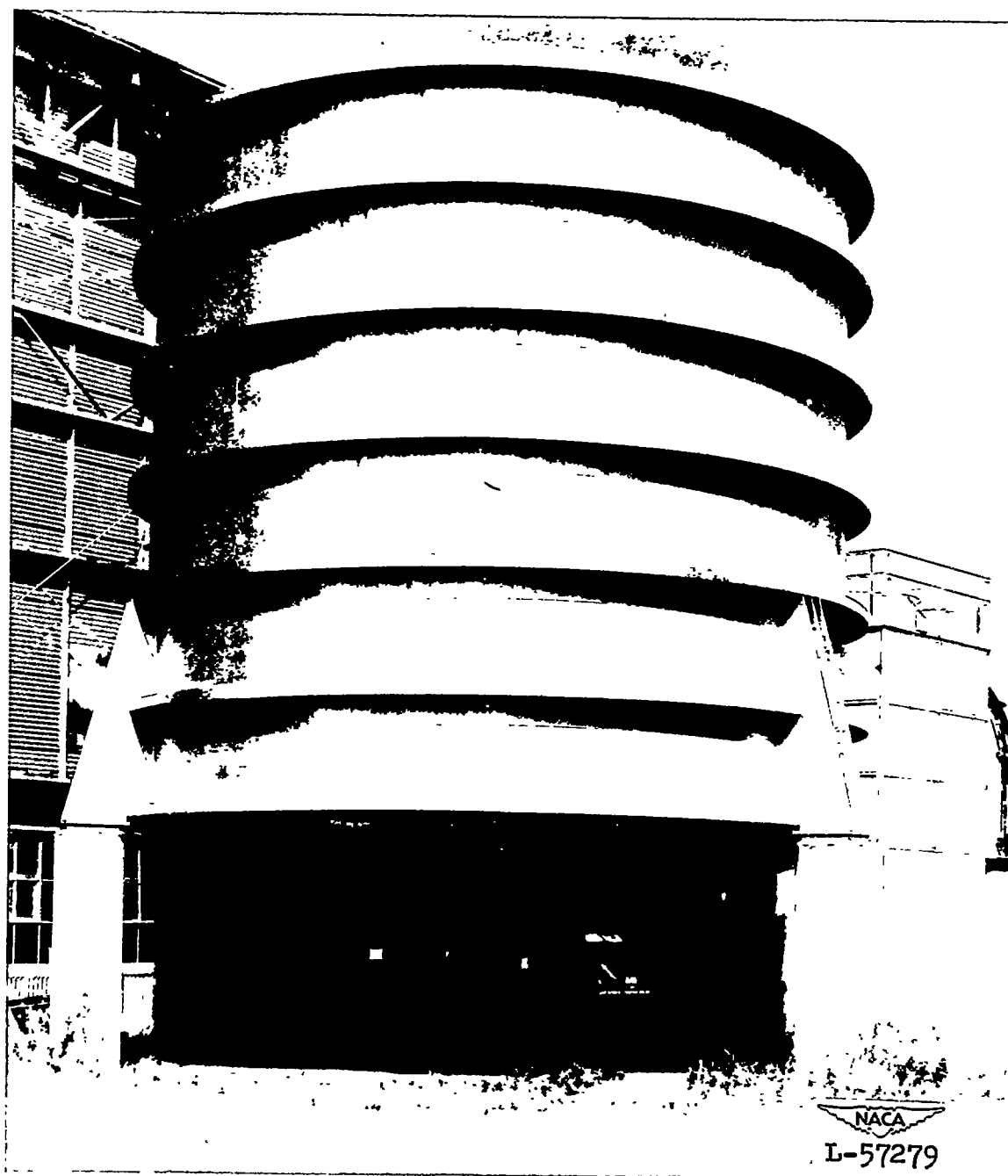
Figure 3.— Vacuum tank.

Figure 4.— View of the tunnel from the heat exchanger to the 24-inch valve.
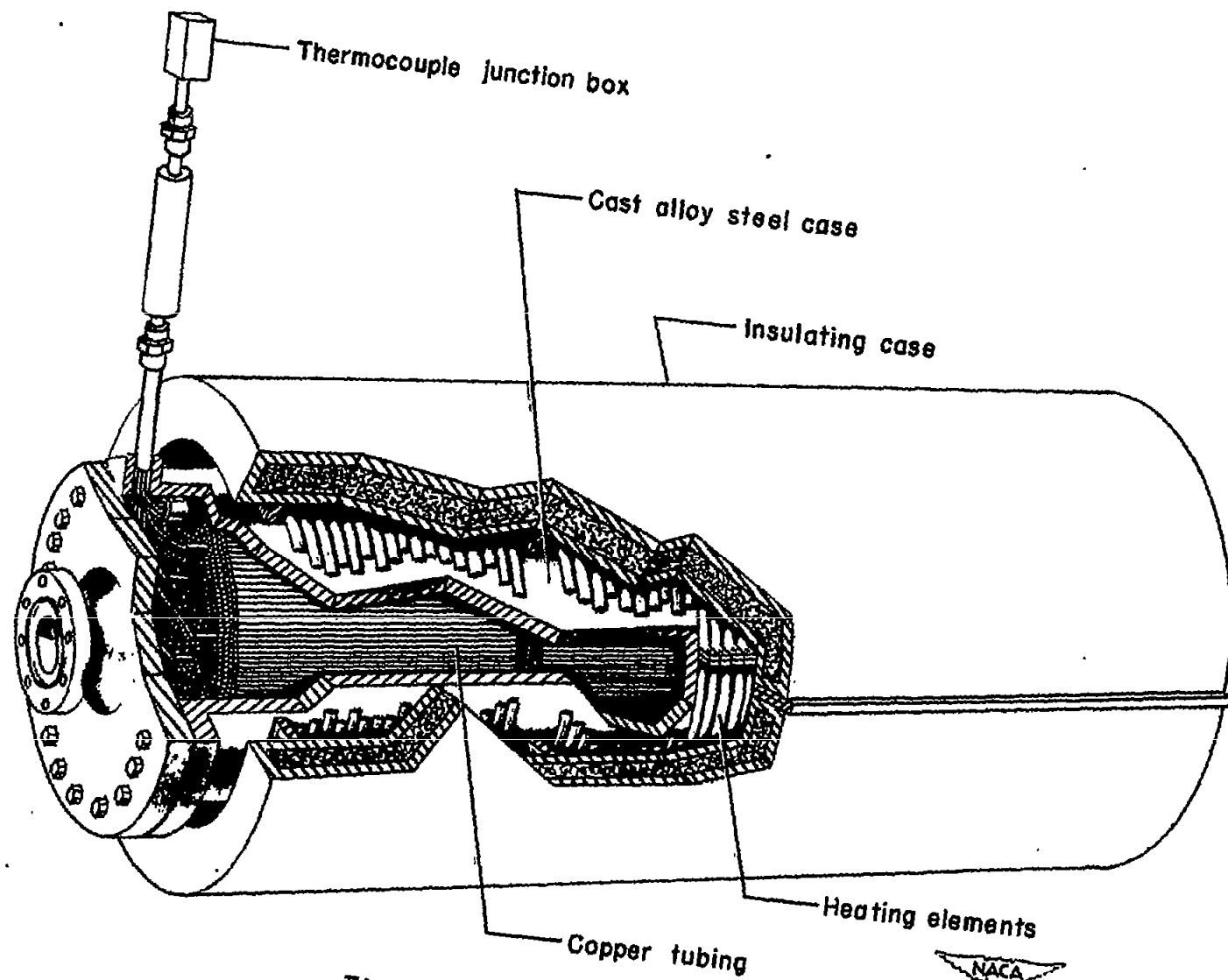
Figure 5.— Cutaway view of heat exchanger.

Thermocouple junction box

Cast alloy steel case

Insulating case

Heating elements

Copper tubing
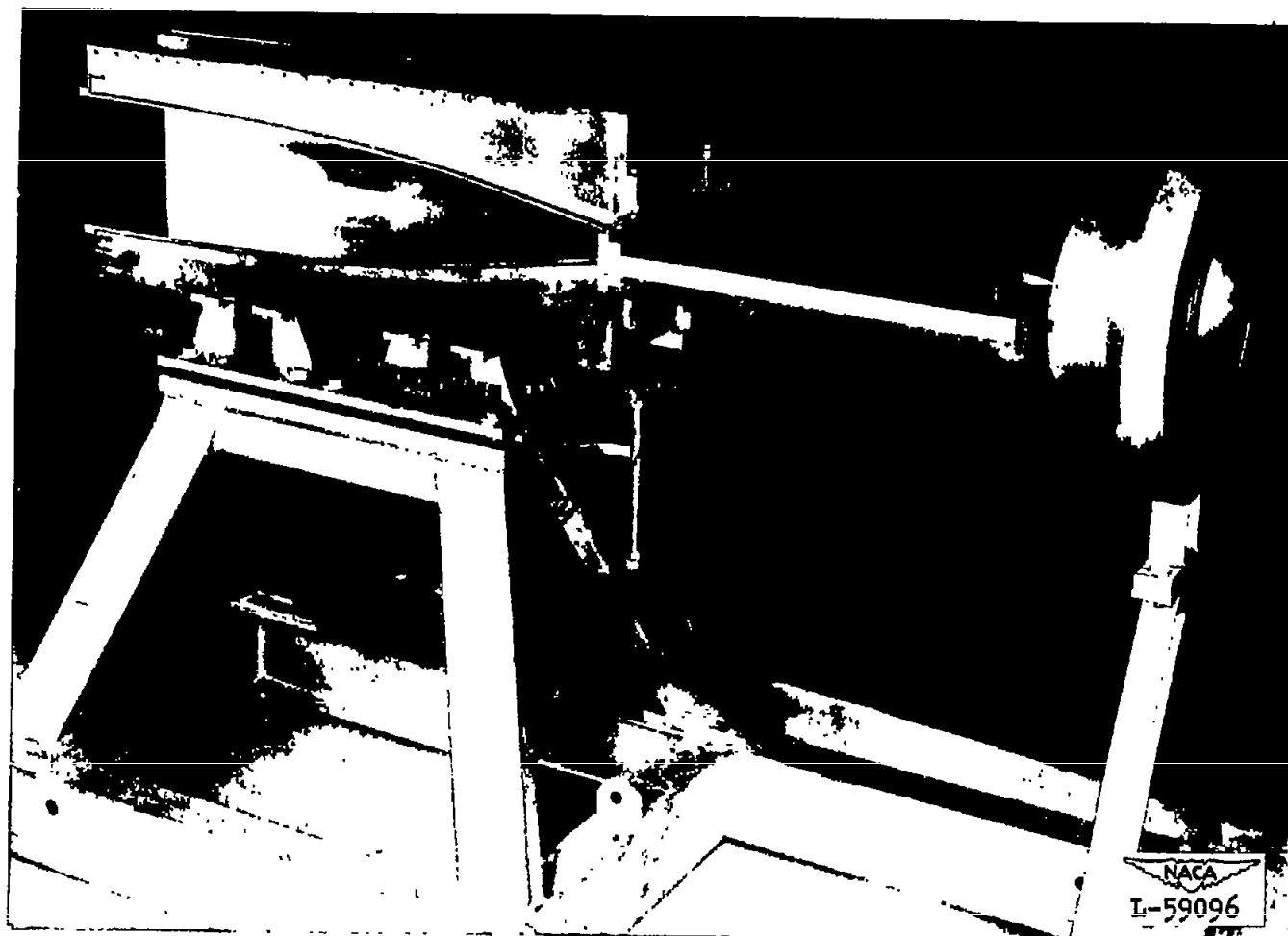
Figure 6.— View of nozzle with top plate of first expansion and side plate of second expansion removed.
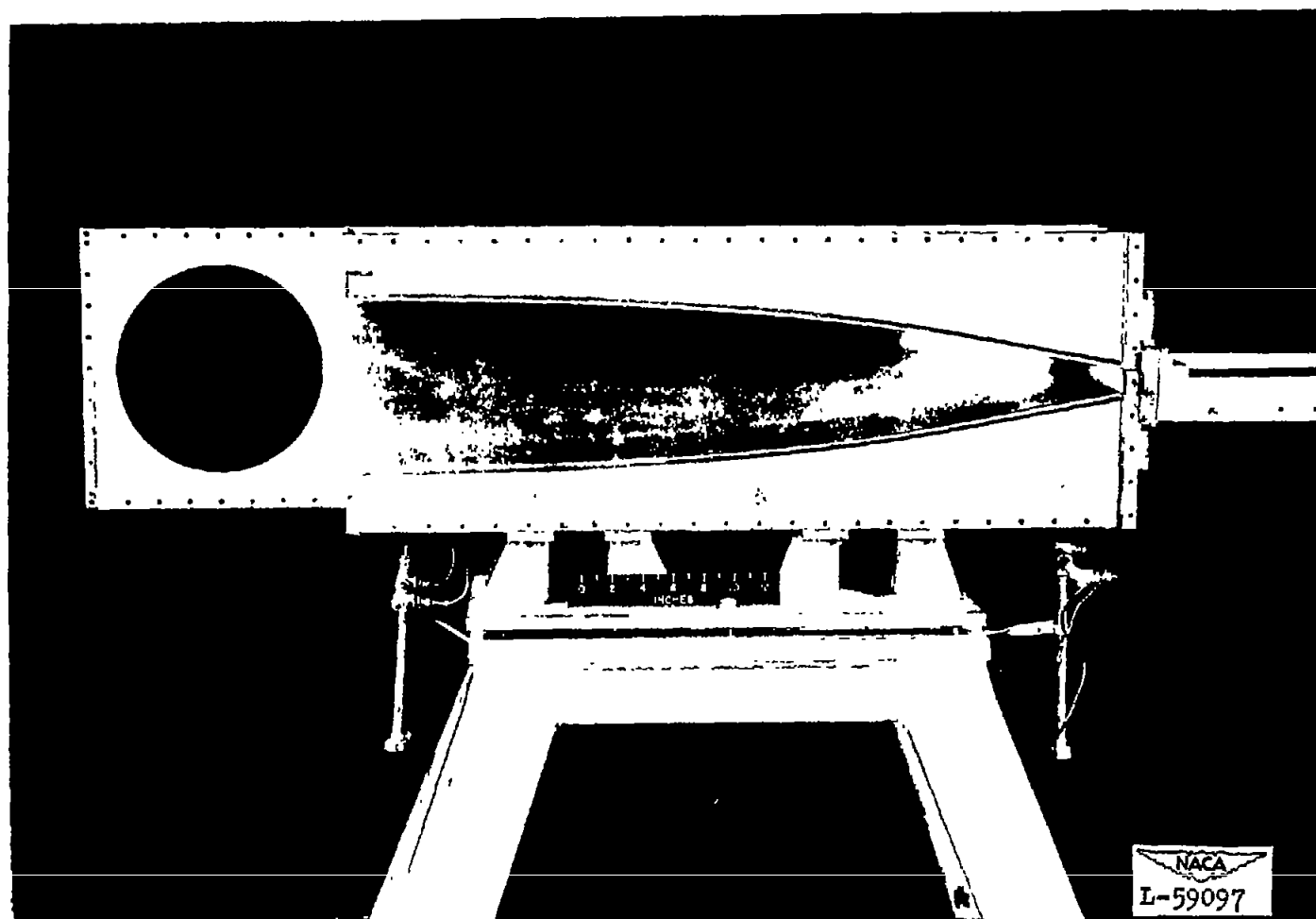
Figure 7.— Second expansion with a side plate removed and test—section side plate with window in place.
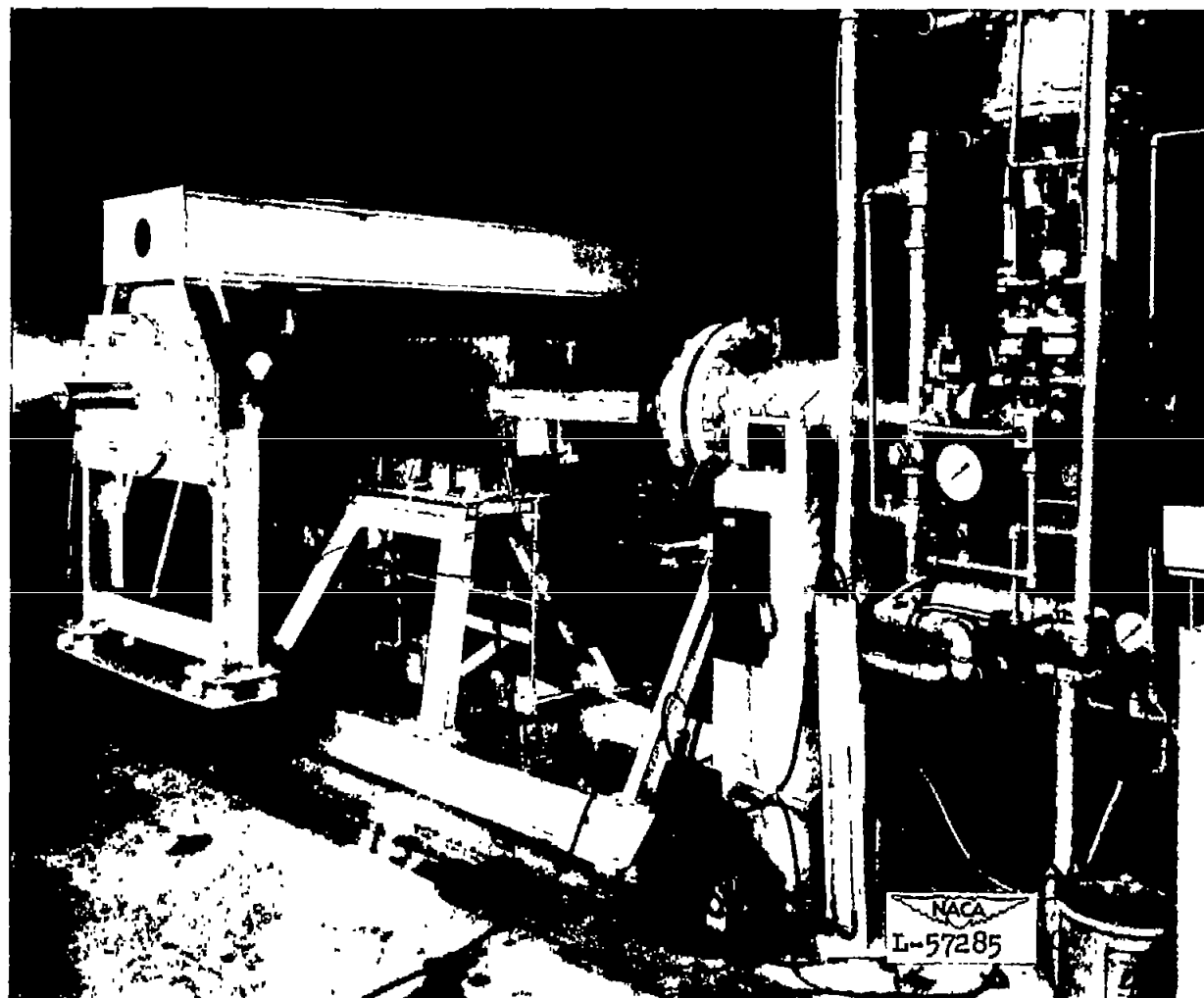
Figure 8.— The nozzle in position in the tunnel.

L-59503
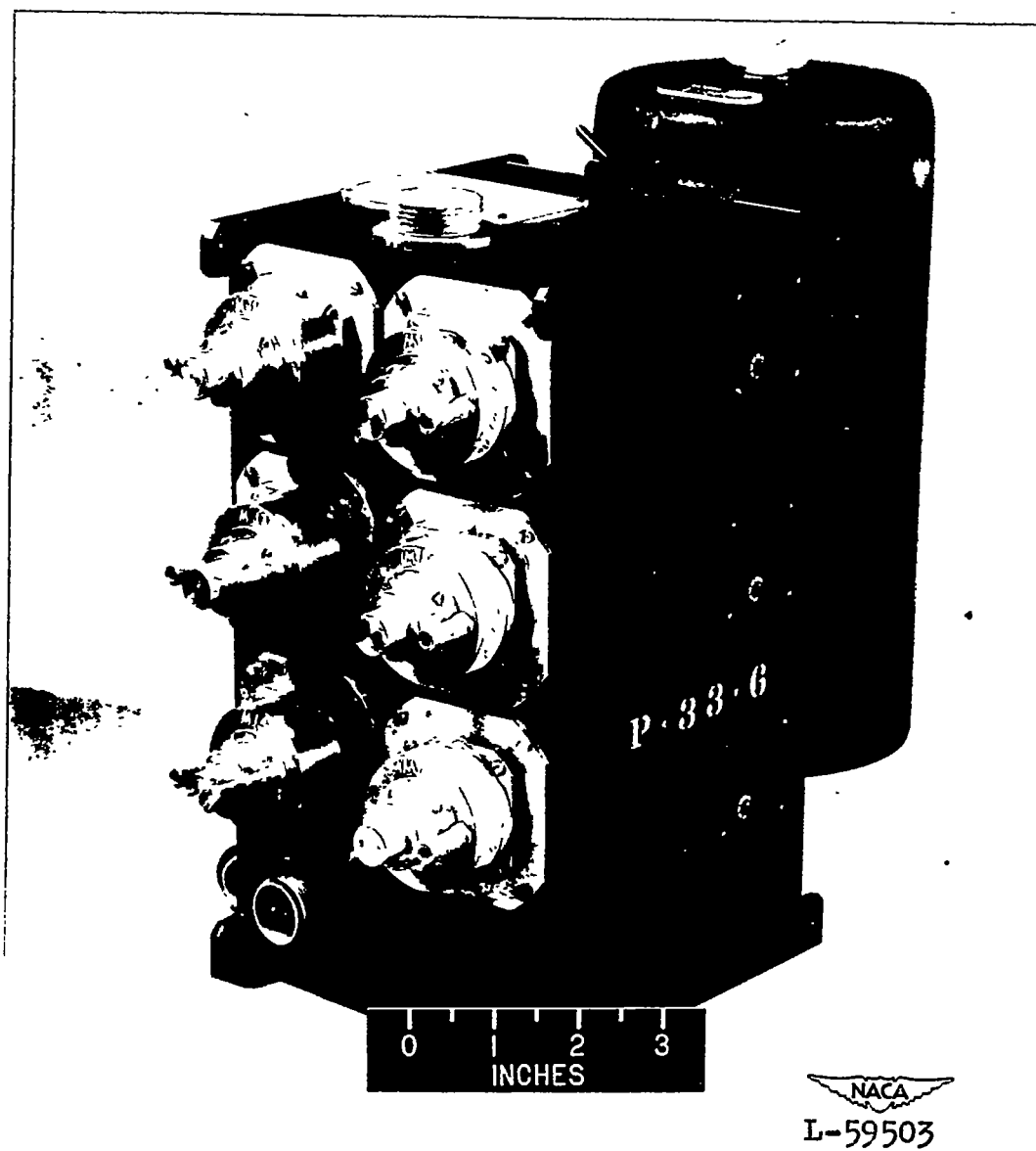
Figure 9.— Six-capsule pressure recorder with film drum in place.

Sensitivity adjustment screws

Mirror staff

Record mirrors

Hairspring

Carriage

Reference mirror

Bridge

Tail

Nesting type
evacuated diaphragm

Zero adjusting screw

Pressure connection
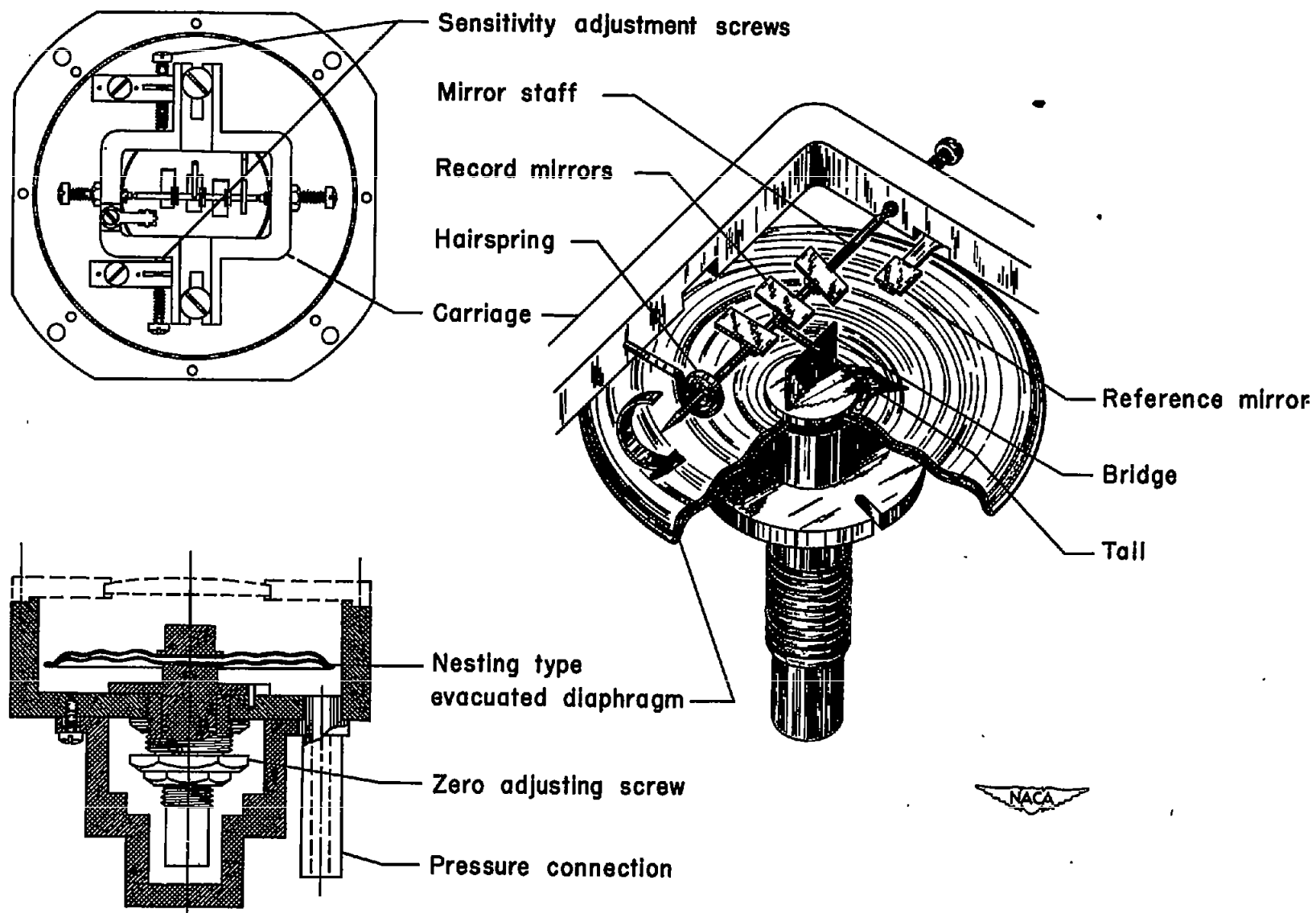
Figure 10.— Low-absolute-pressure capsule.

High-pressure mercury-vapor light source

Condensing lens

Mirror knife edge

Test section

Shielding tube

Spherical mirror 12 in. diam.

Automatic camera

Knife edge

— 20 feet —

Arrangement for horizontal viewing

NACA

Plane mirror

Arrangement for vertical viewing
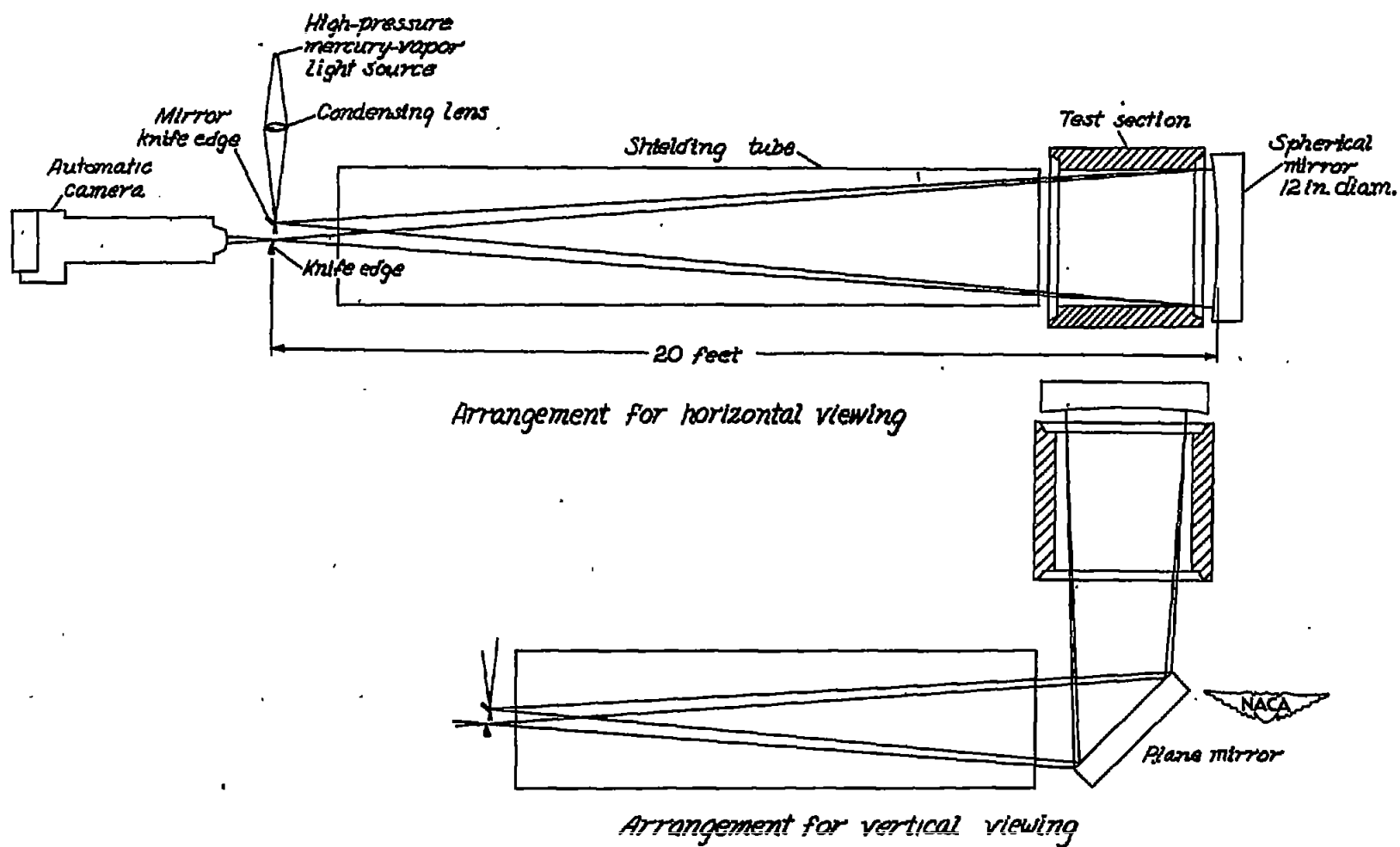
Figure 11.— Schematic representation of the schlieren apparatus.
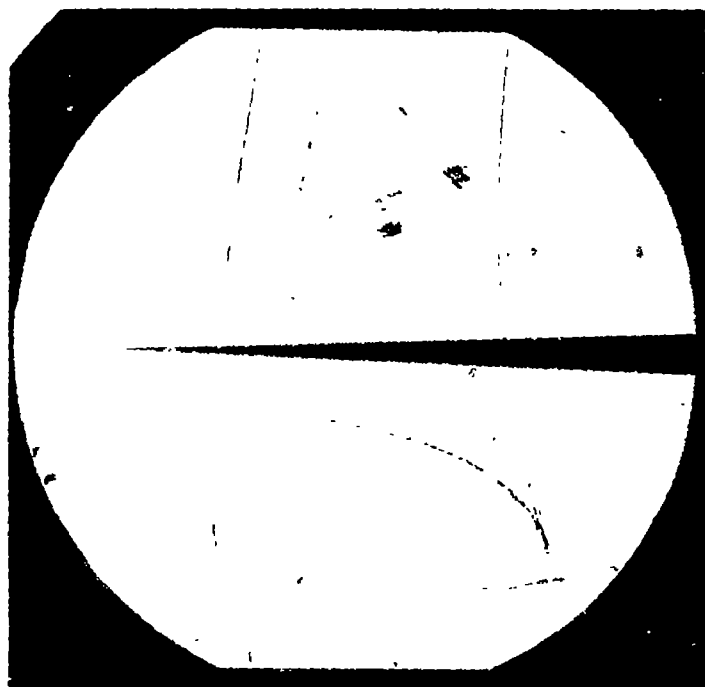
(a) No flow.
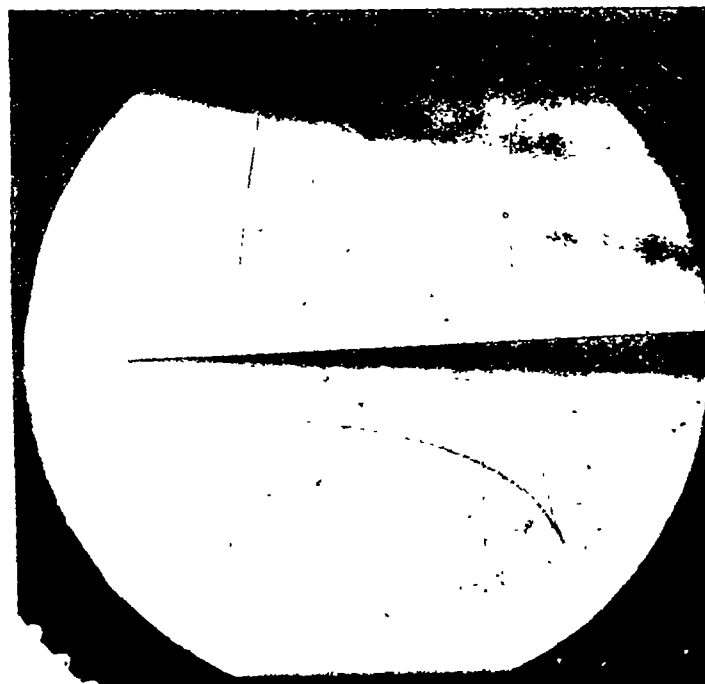
(b) M equal approximately 6.5. L-60578

Figure 12.— Schlieren photographs of a 4° cone.
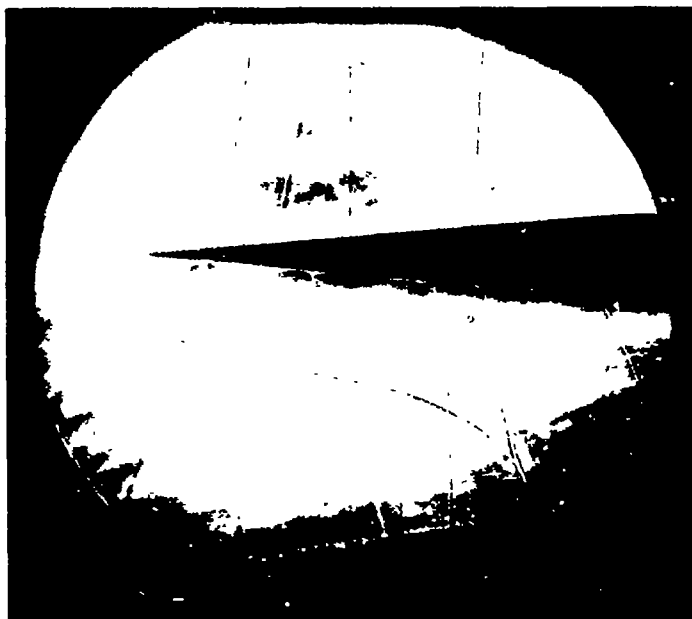
(a) No flow.
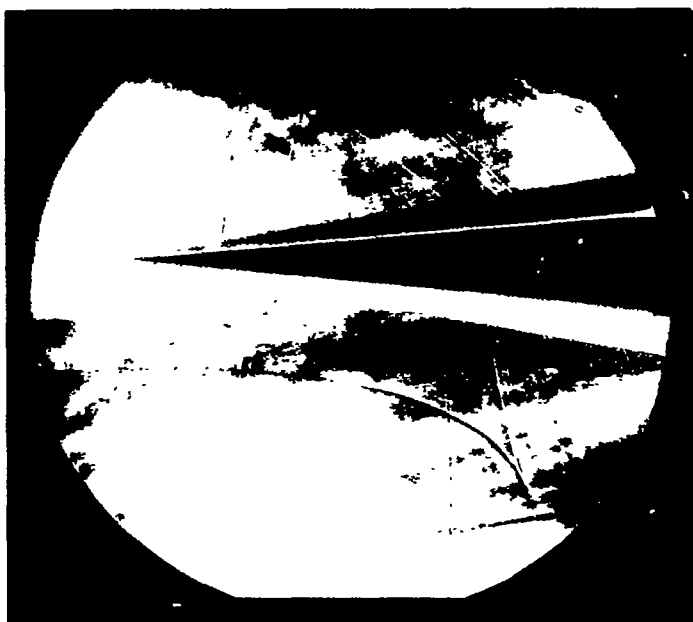
(b) M equal approximately 6.5. L-60579

Figure 13.— Schlieren photographs of a 10° cone.
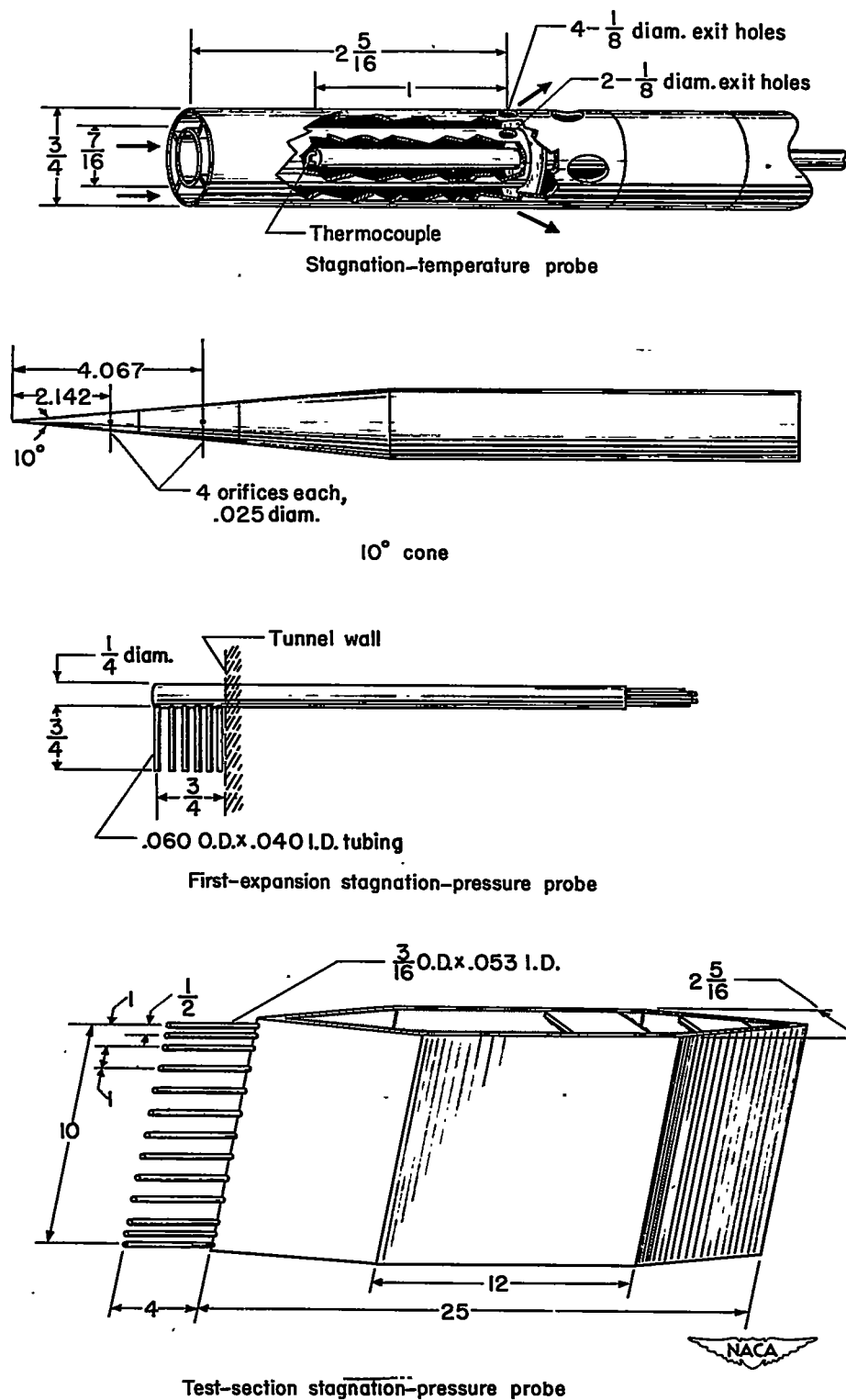
Figure 14.— Survey probes. (All dimensions are in inches.)
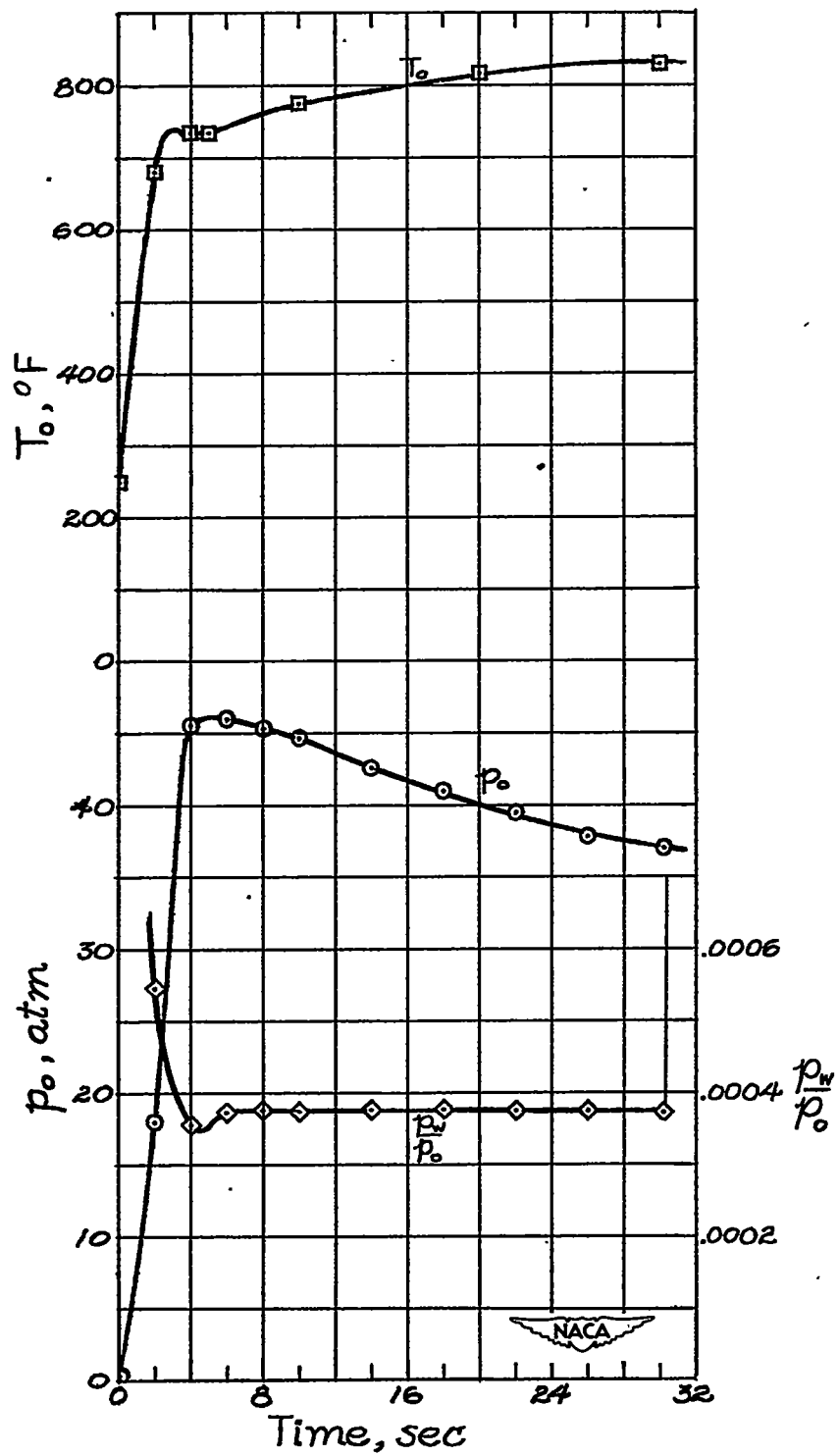
Figure 15.— Results from a typical test.
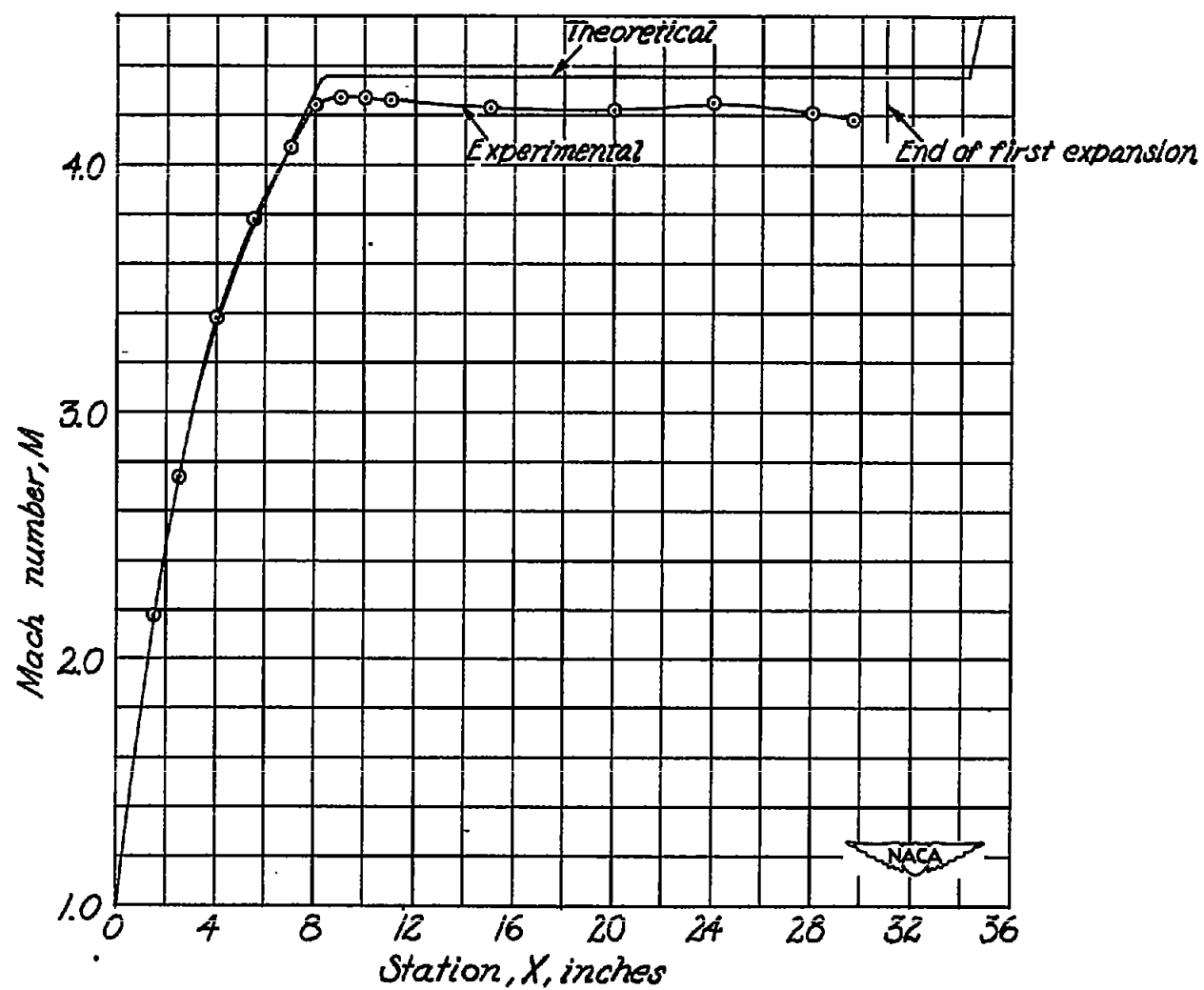
Figure 16.— Variation of Mach number along the longitudinal center line of the first-expansion wall.
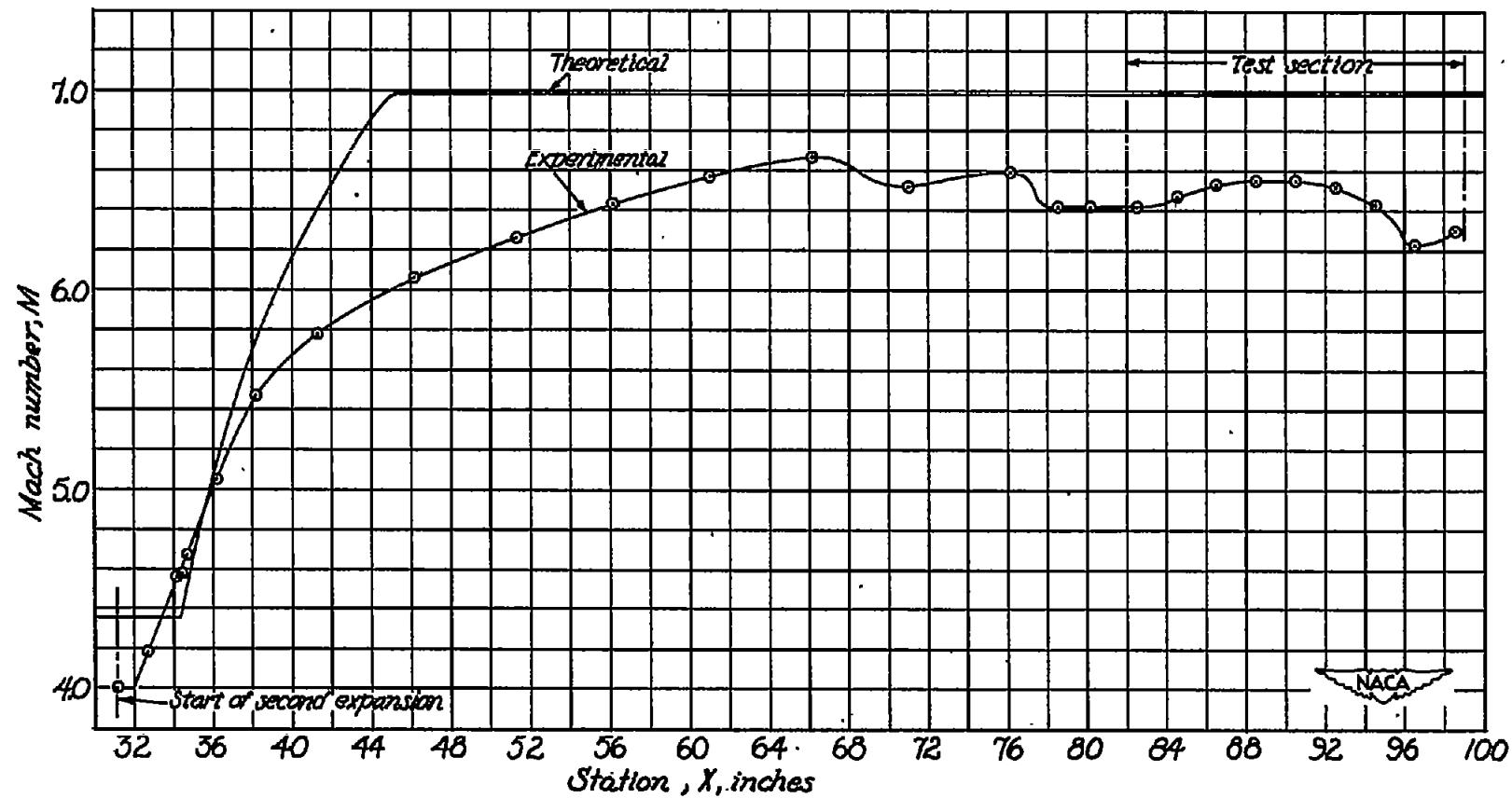
Figure 17.— Variation of Mach number along the longitudinal center line of the second-expansion wall.
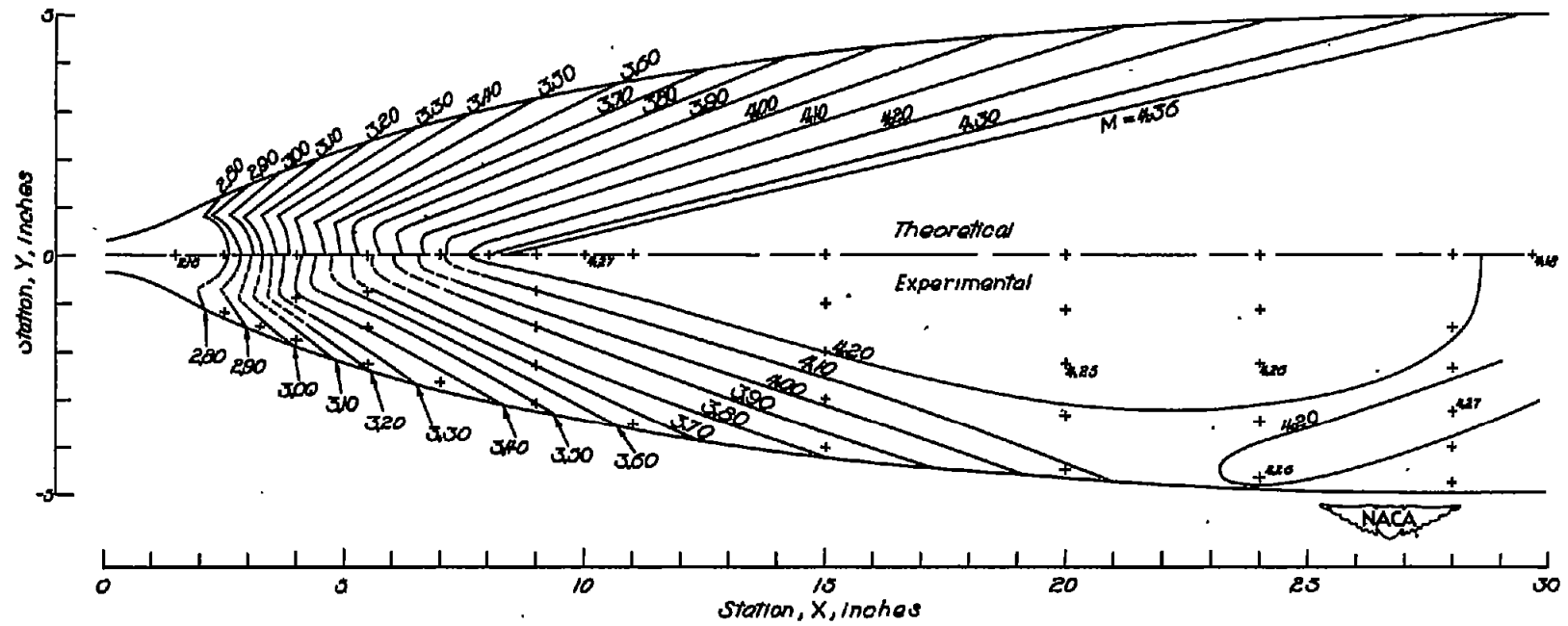
Figure 18.— Mach number contours in the first expansion.

Figure 19.— Mach number contours in the second expansion.

(a) Shock patterns (approx. 4 microsec exposure).
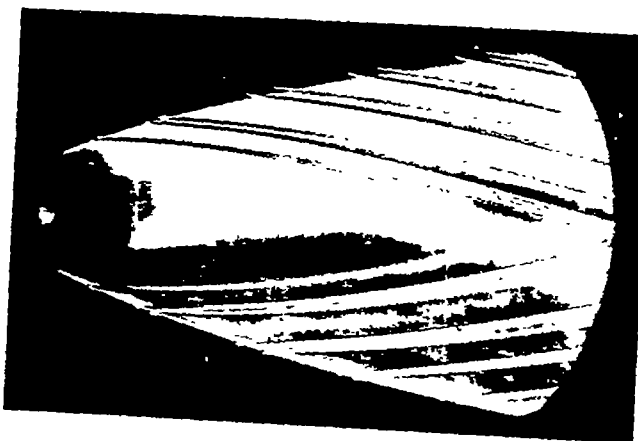
(b) Shock patterns (1/50 sec exposure).

(c) No flow.

L-60577

Figure 20.— Schlieren photographs of a portion of the first expansion.
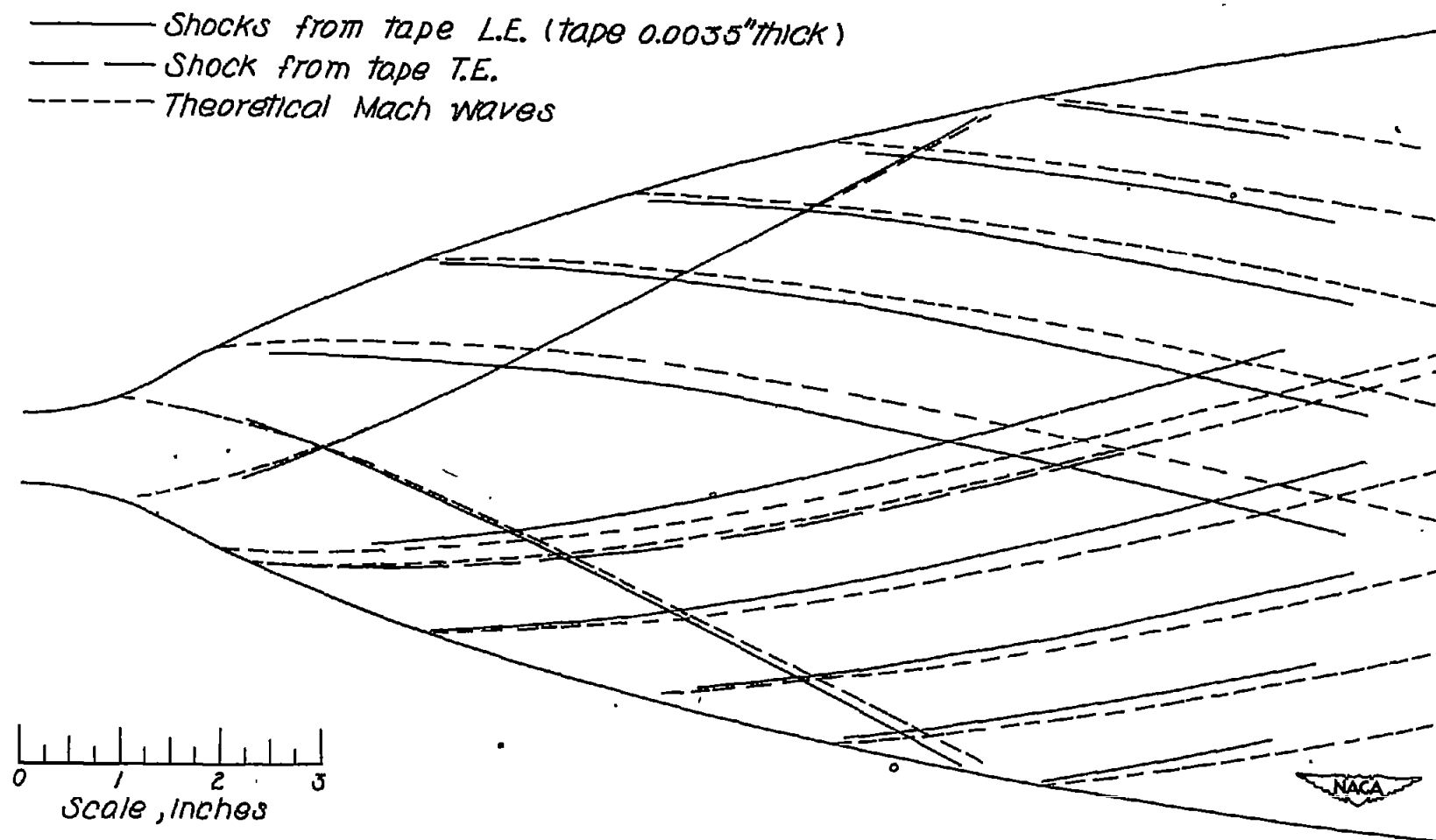
Figure 21.— Comparison of theoretical Mach waves with weak shocks in the first expansion.
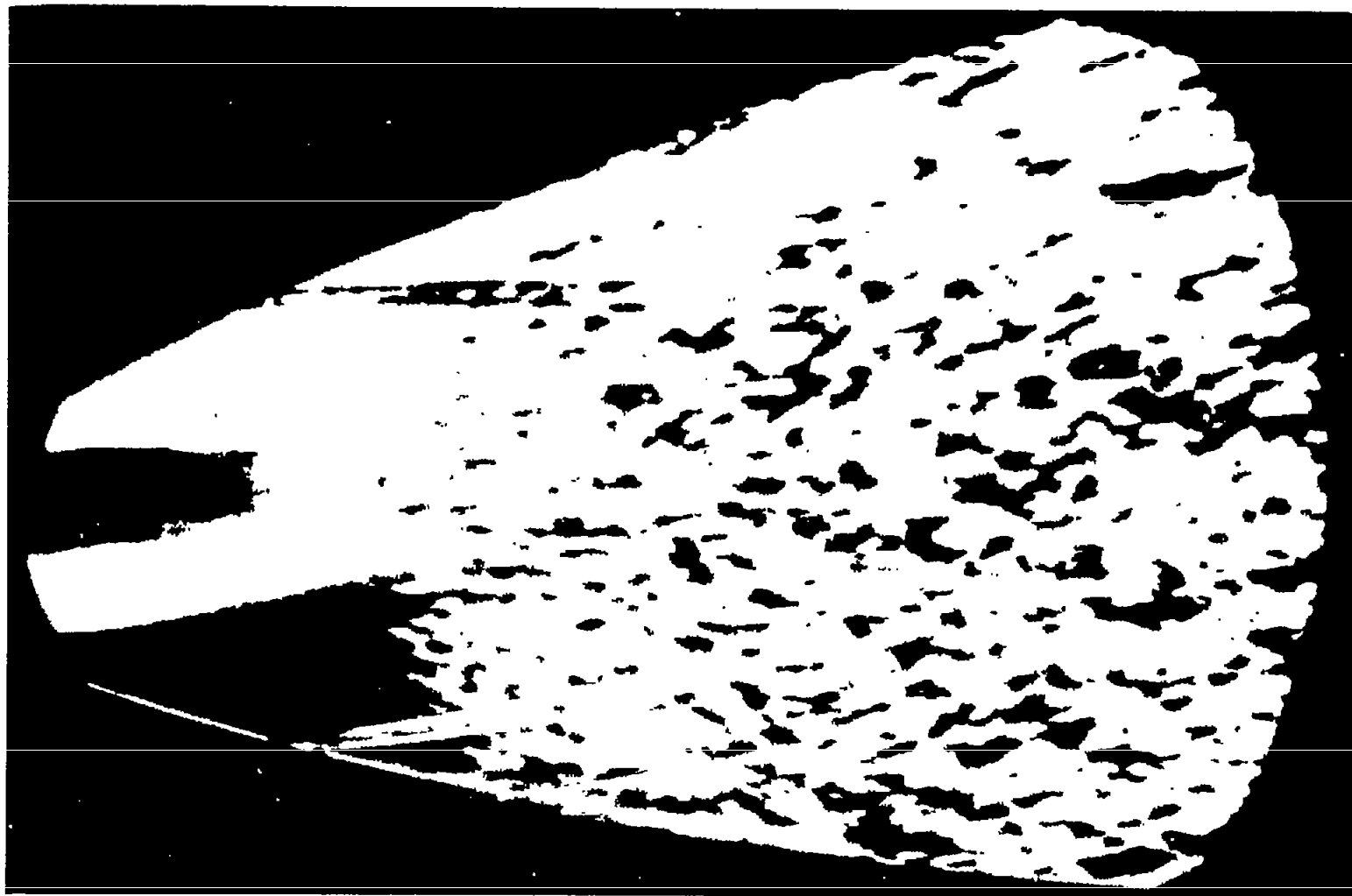
L-60580

Figure 22.— Schlieren photograph of the breakdown of supersonic flow in the first expansion.
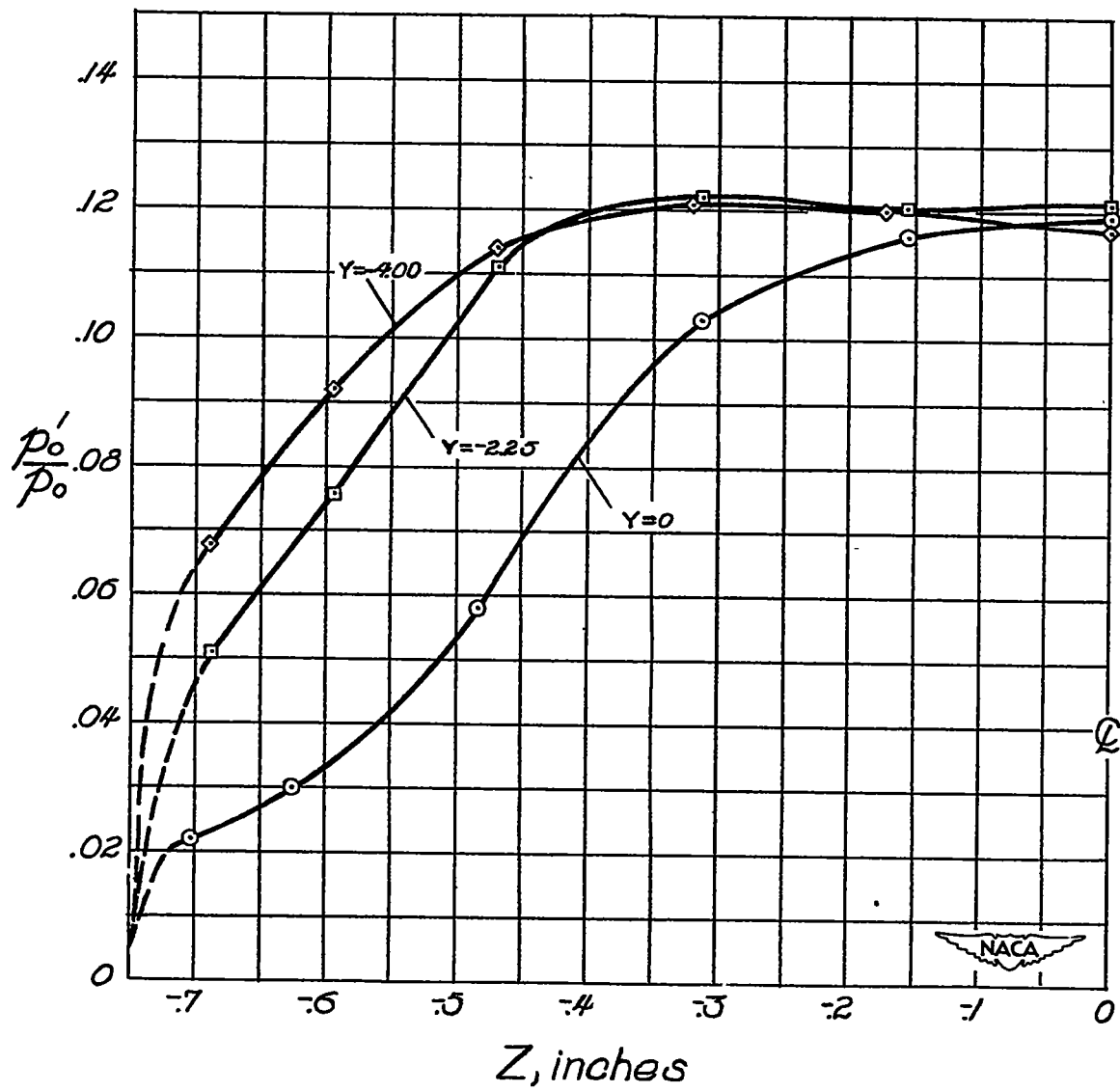
Figure 23.— Pressure recovery at station 26.9 in the first expansion.
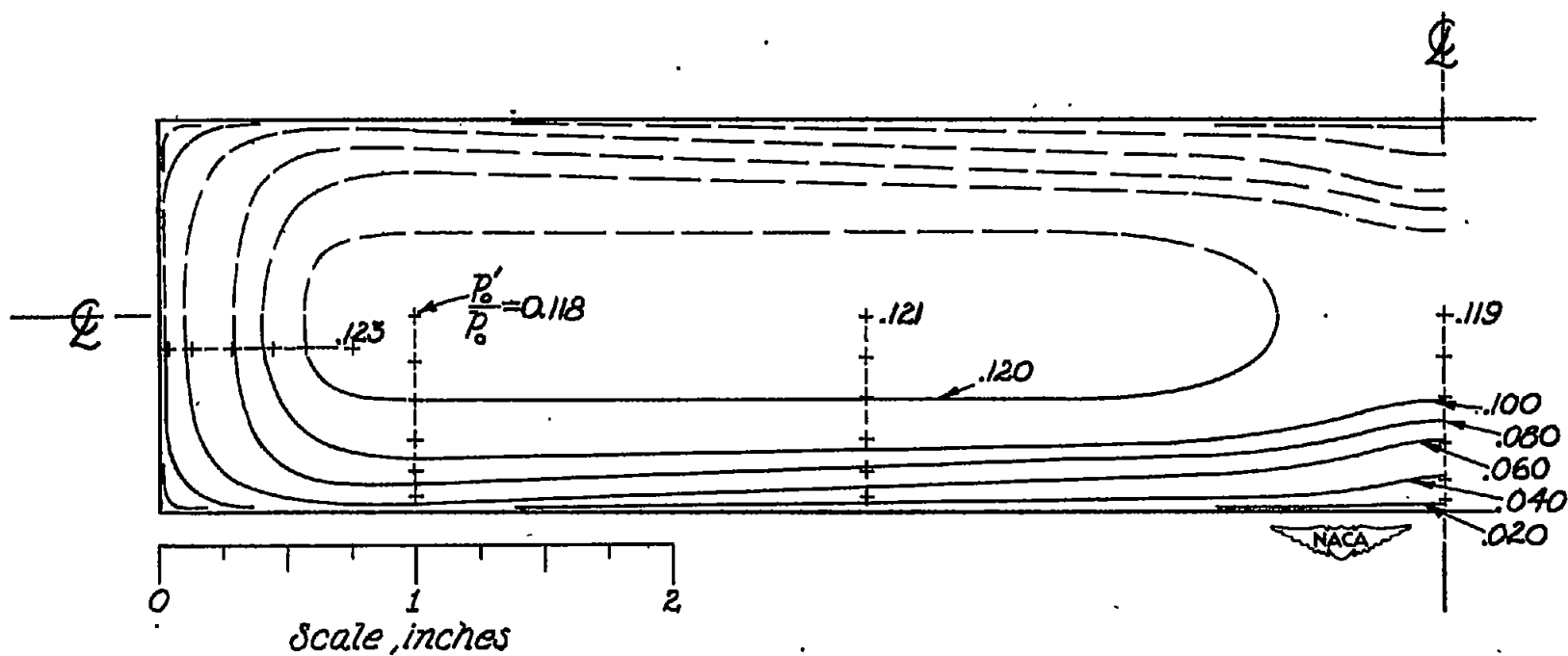
Figure 24.— Pressure-recovery contours at $X = 26.9$ in the first expansion (upstream view).
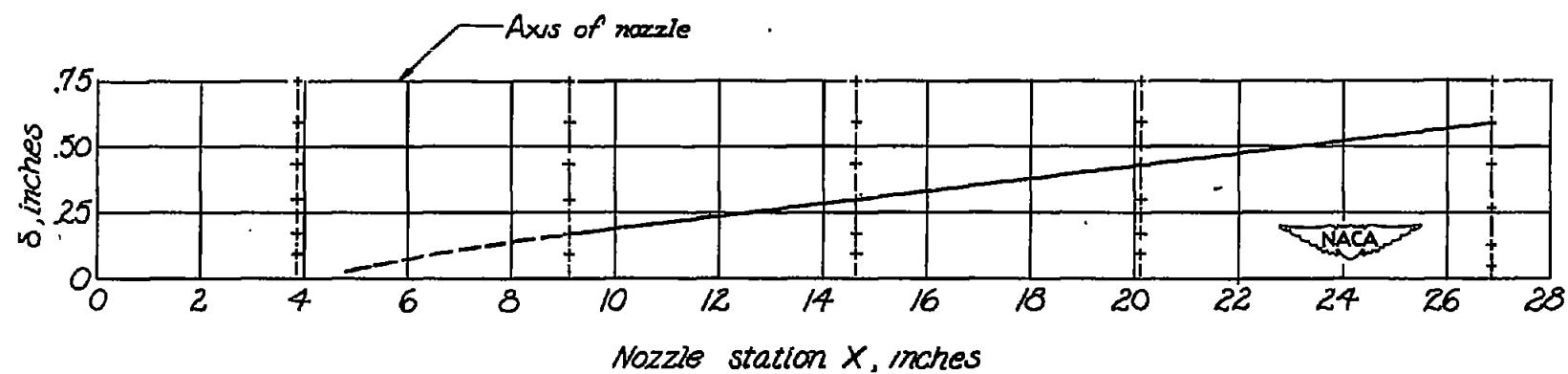
Figure 25.— Boundary-layer growth along the center line of the parallel walls in the first expansion.
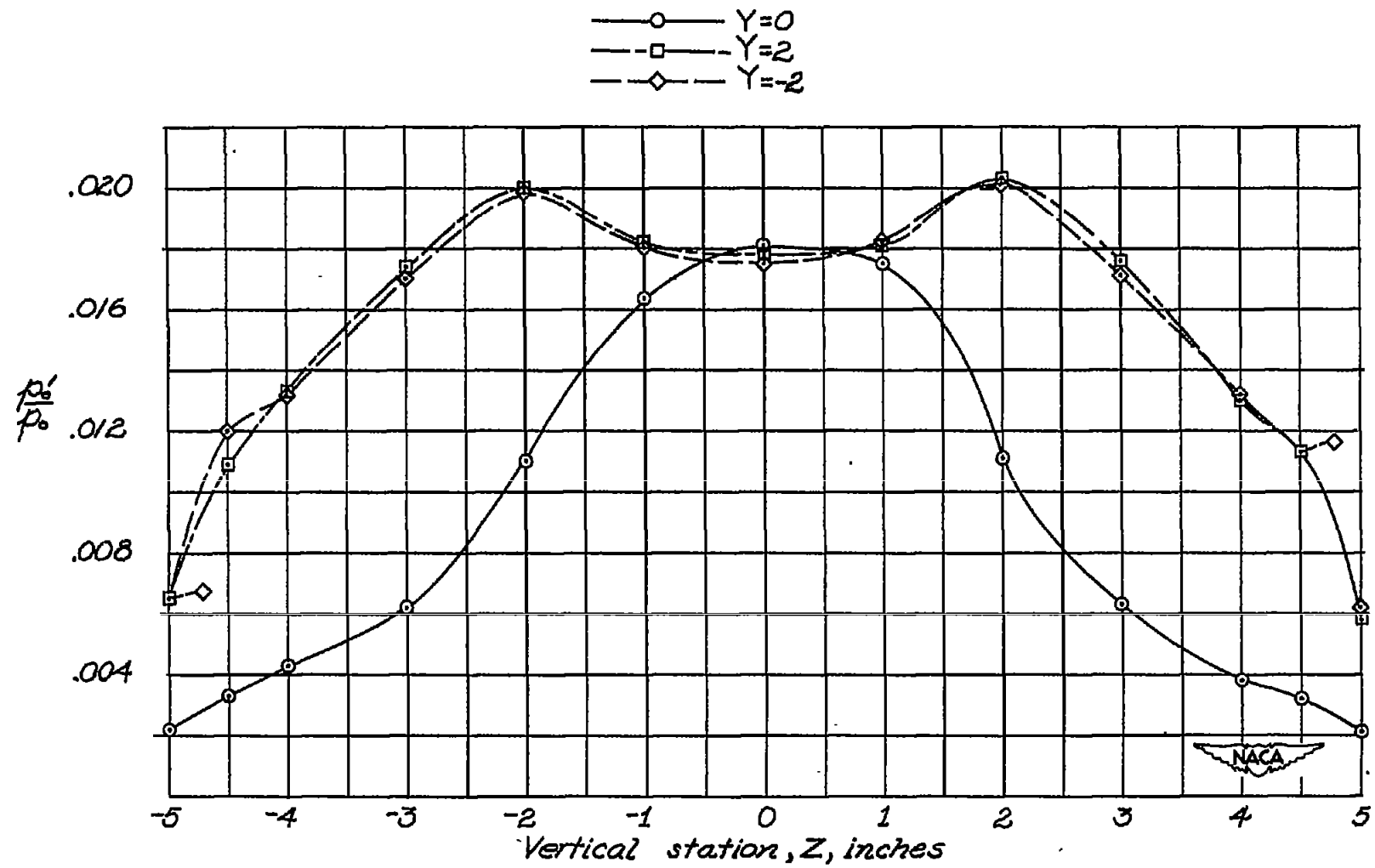
Figure 26.— Comparison of pressure recovery with vertical station at three points across the width of the test section at X = 89.7.
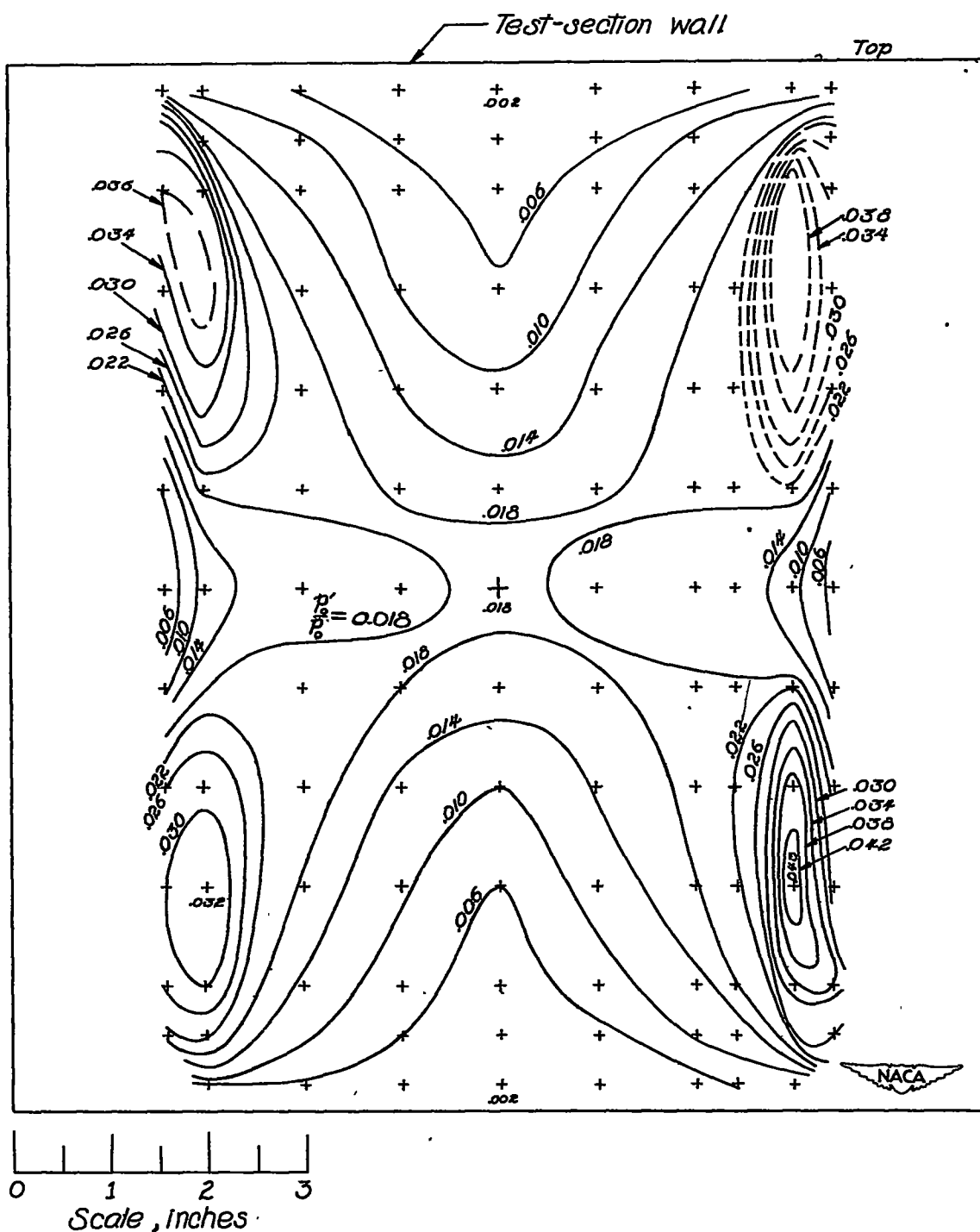
Figure 27.— Pressure-recovery contours at station 89.7 in the test
section (upstream view).
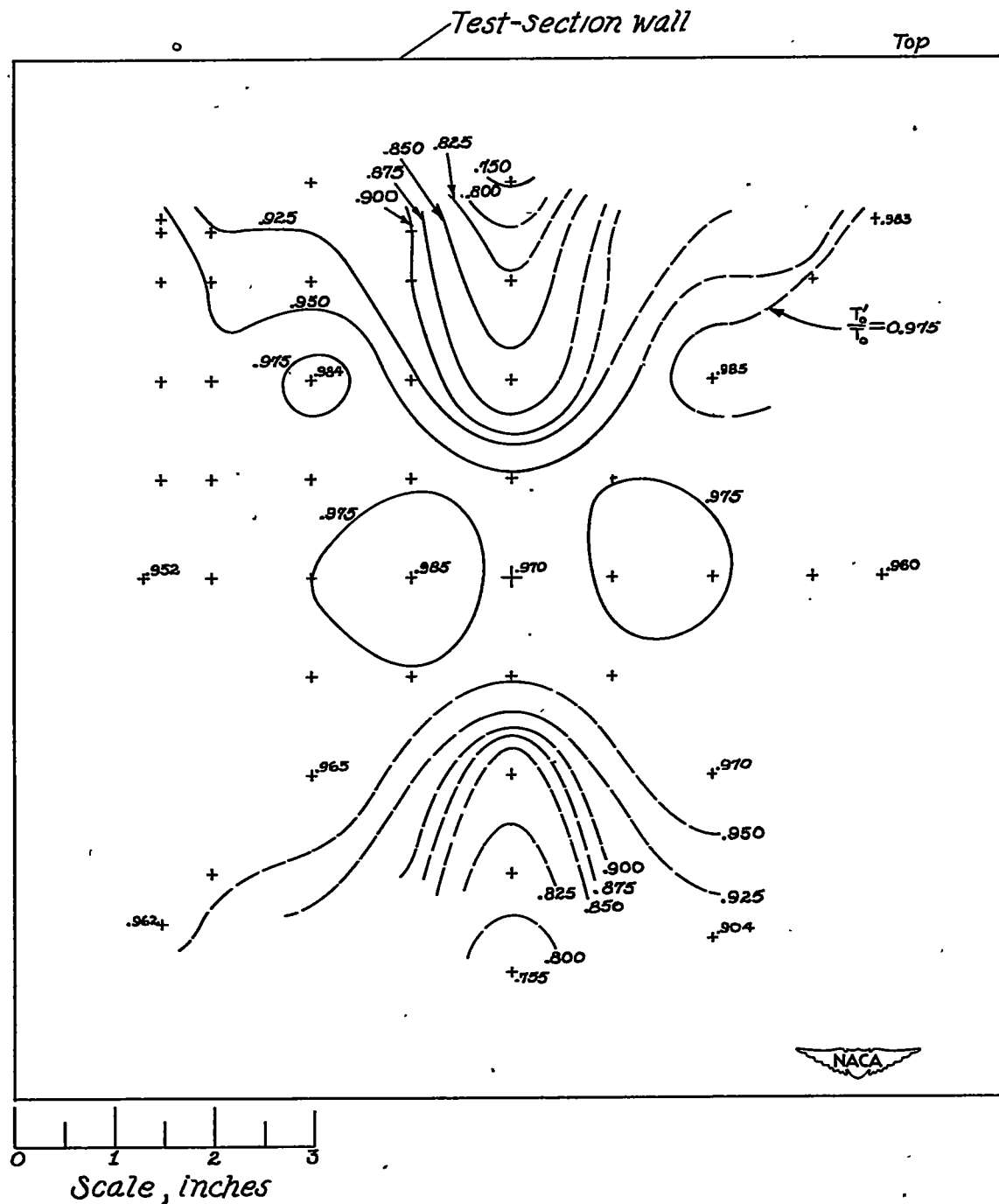
Figure 28.— Temperature-recovery-factor contours at station 90.9 in the test section (upstream view).
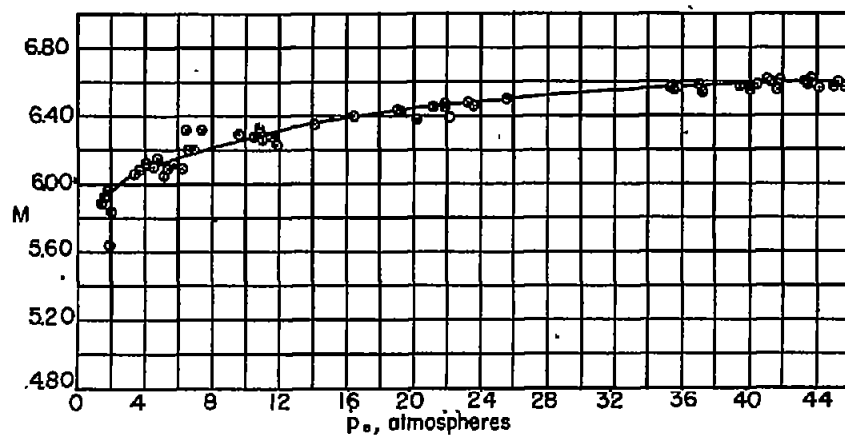
(a) Station 76.14.
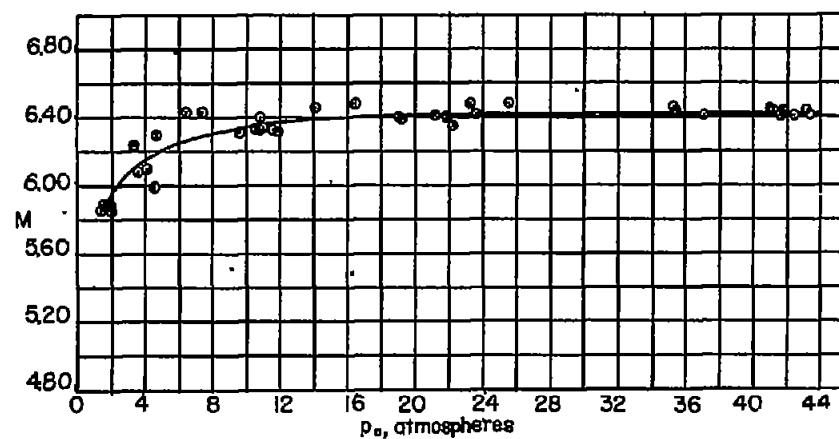
(b) Station 82.5.
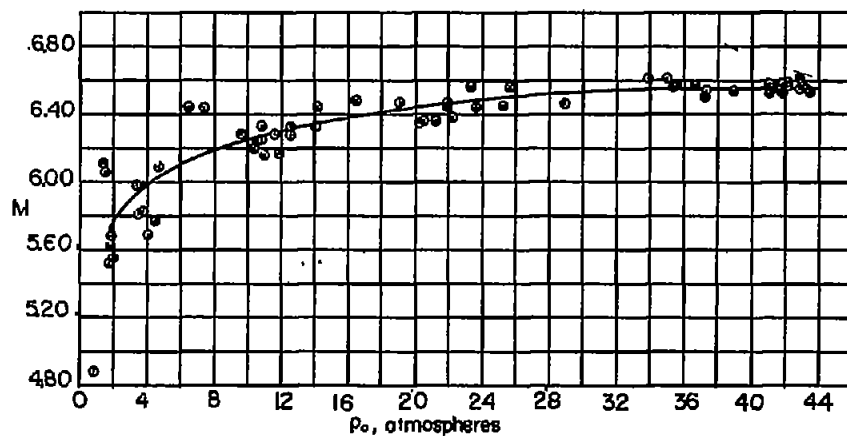
(c) Station 90.5.
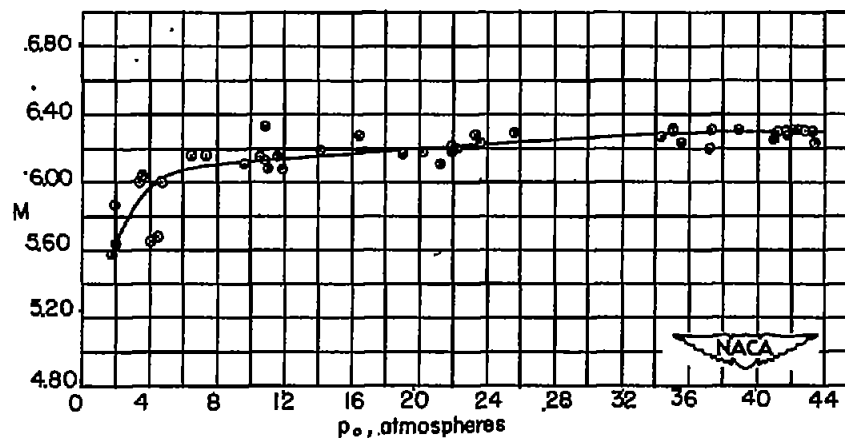
(d) Station 98.5.

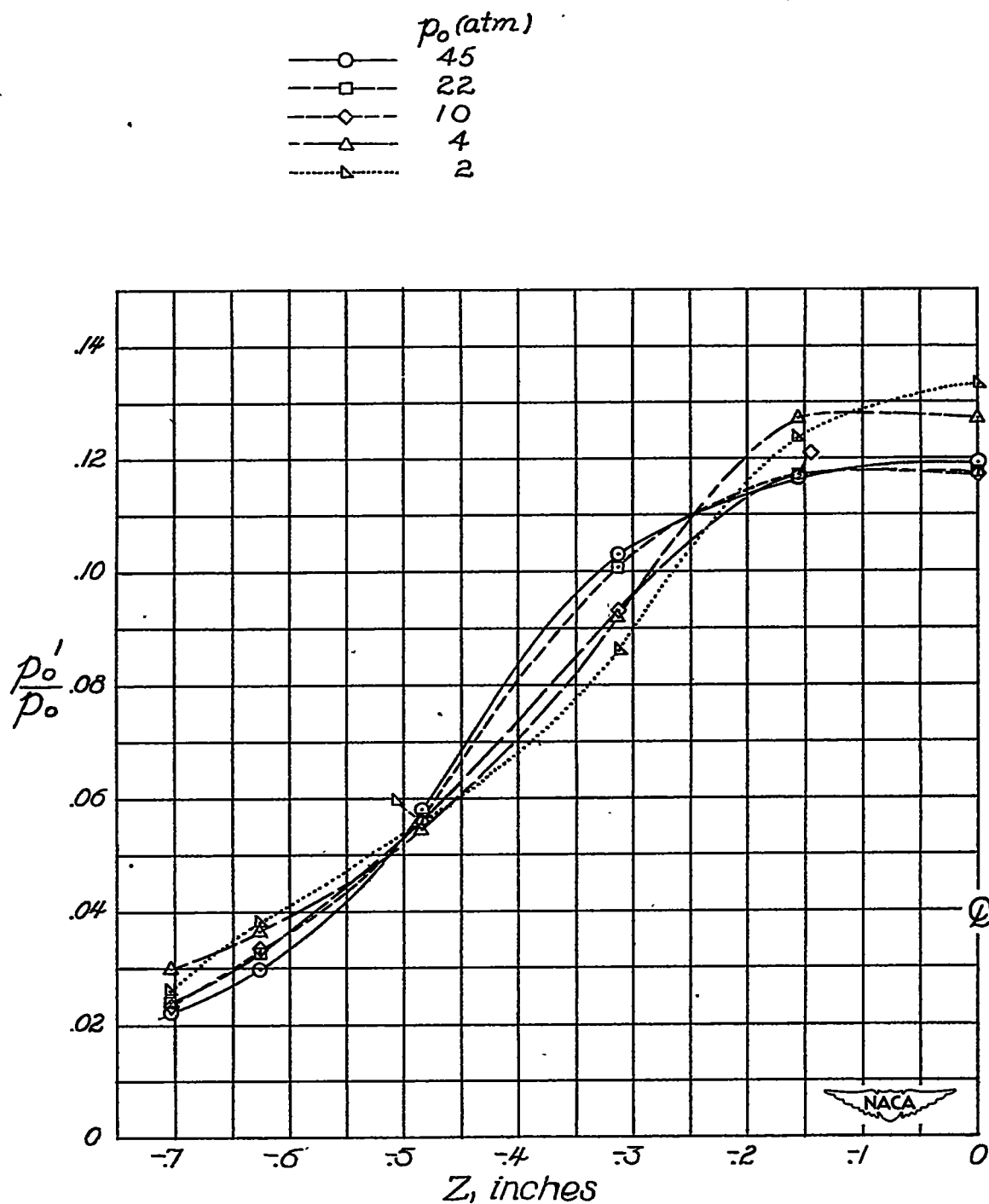Figure 29.— The variation of indicated Mach number with settling-chamber pressure.

Figure 30.— Effect of settling-chamber pressure on the stagnation
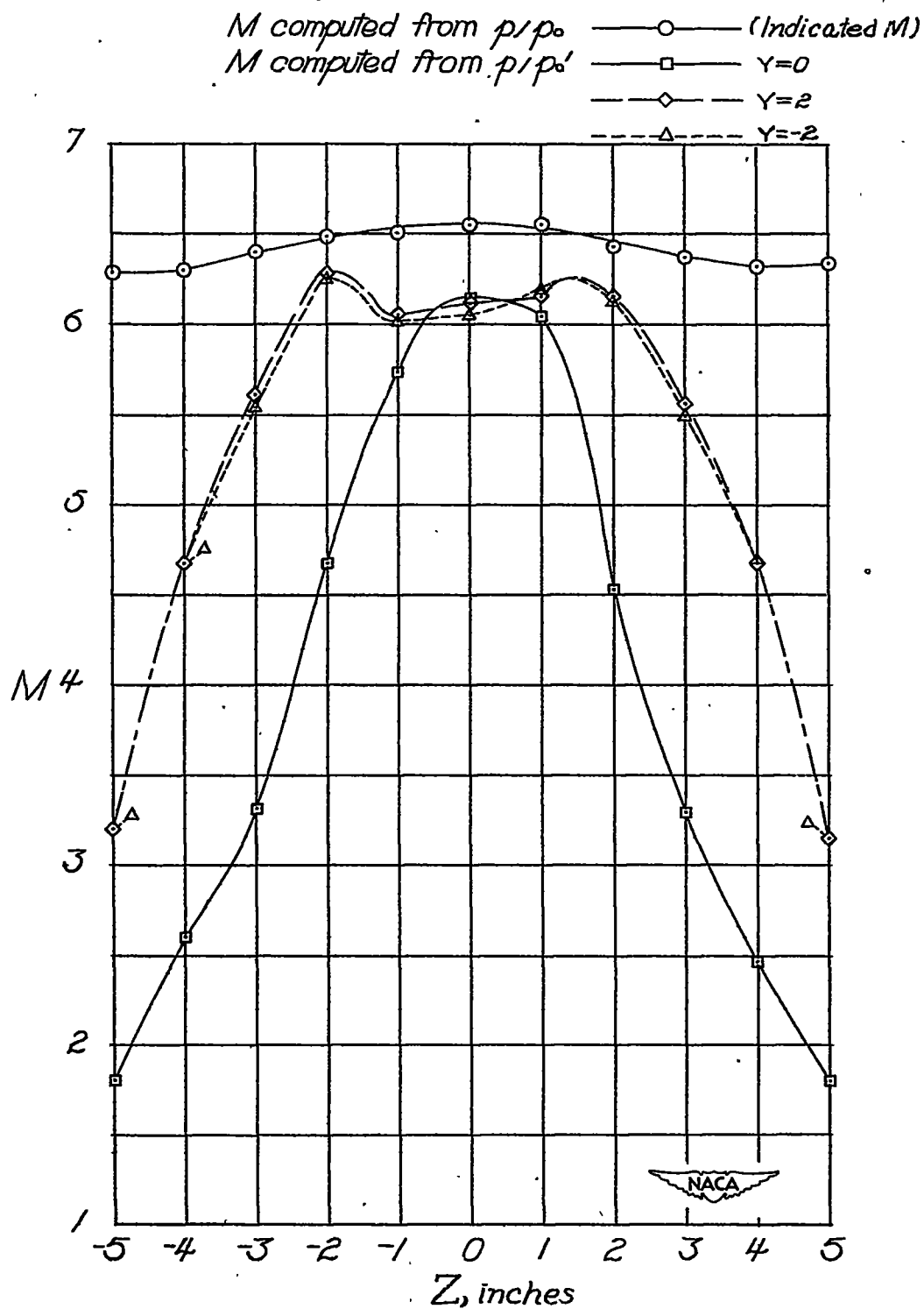pressure in the first expansion at Z = 0 and station 26.9.

Figure 31.— Comparison of Mach number distributions at station 90.5
calculated from static pressures assuming isentropic flow and
those based on static pressure and pressure recoveries.

M computed from p/p_o' ──o──
M computed from p_δ/p_o' ──□─o──
M computed from shock measurements (10°cone) ──────
M computed from shock measurements (4°cone) ············

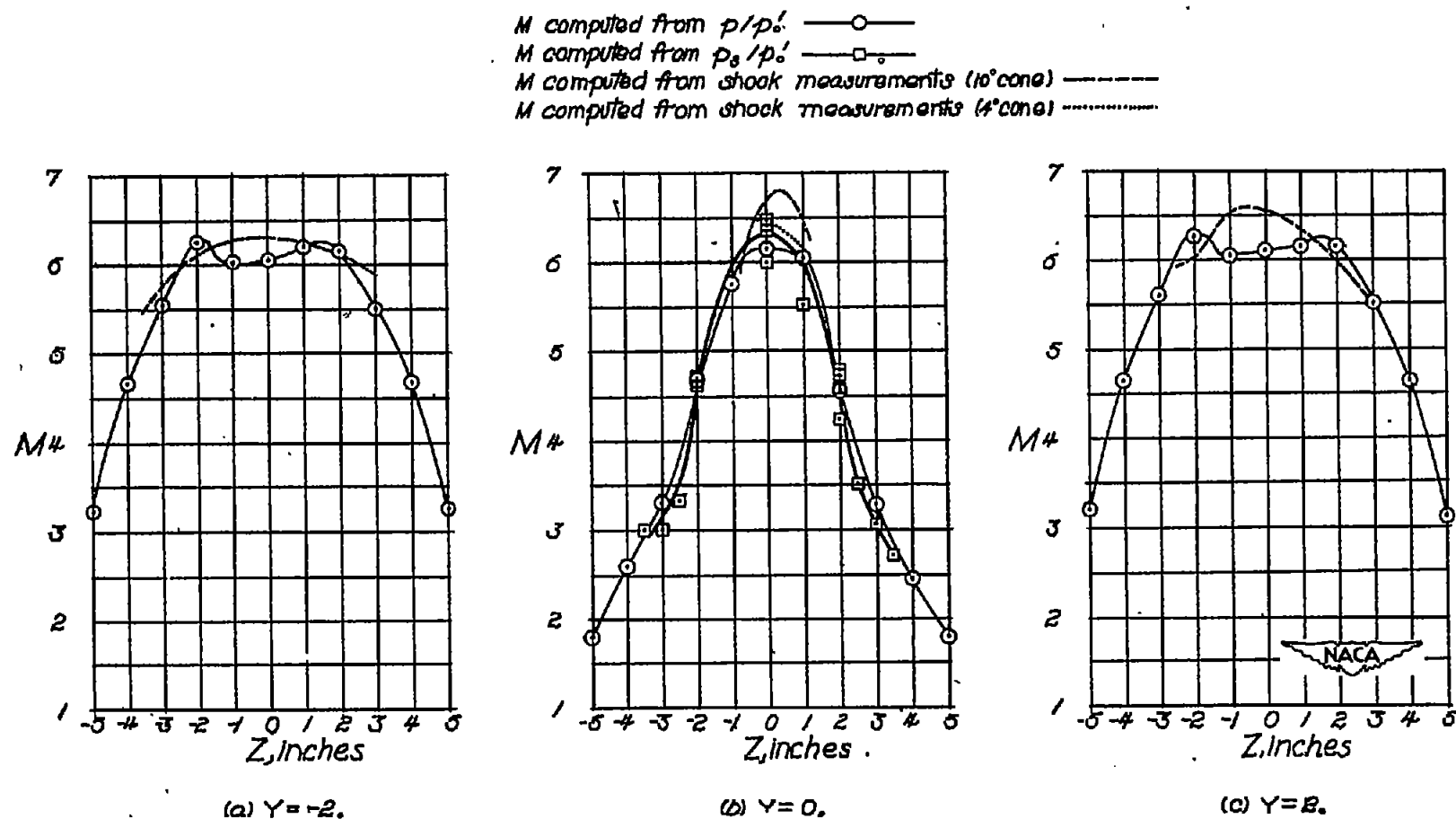(a) Y = -2.   (b) Y = 0.   (c) Y = 2.

Figure 32.— Vertical survey of Mach numbers at station 90.5 by various methods.
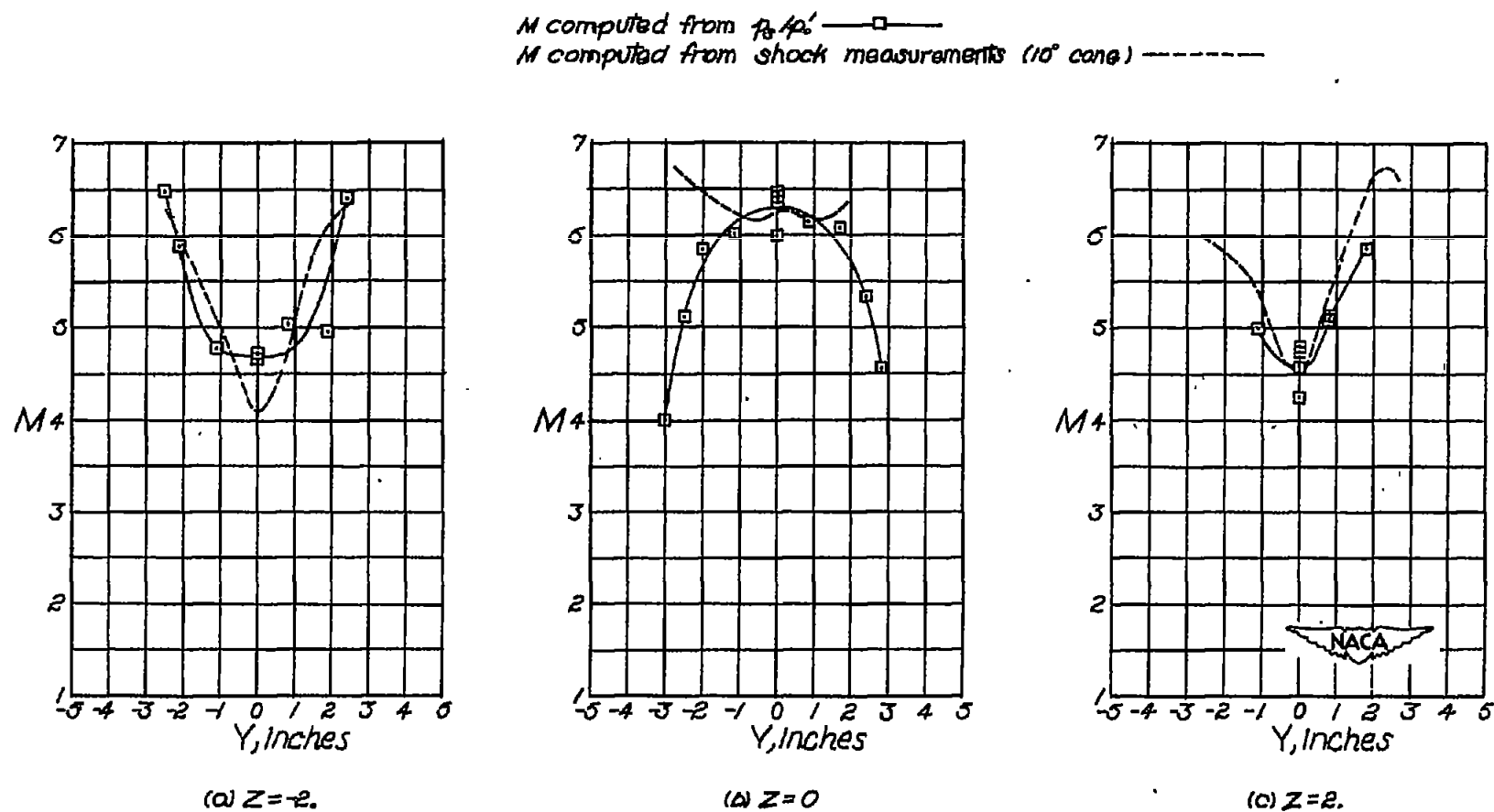
Figure 33.— Horizontal survey of Mach numbers at station 90.5.

ϵ computed from cone-surface-pressure measurements ϵ_v —△—

ϵ computed from shock-angle measurements (10°cone) ------
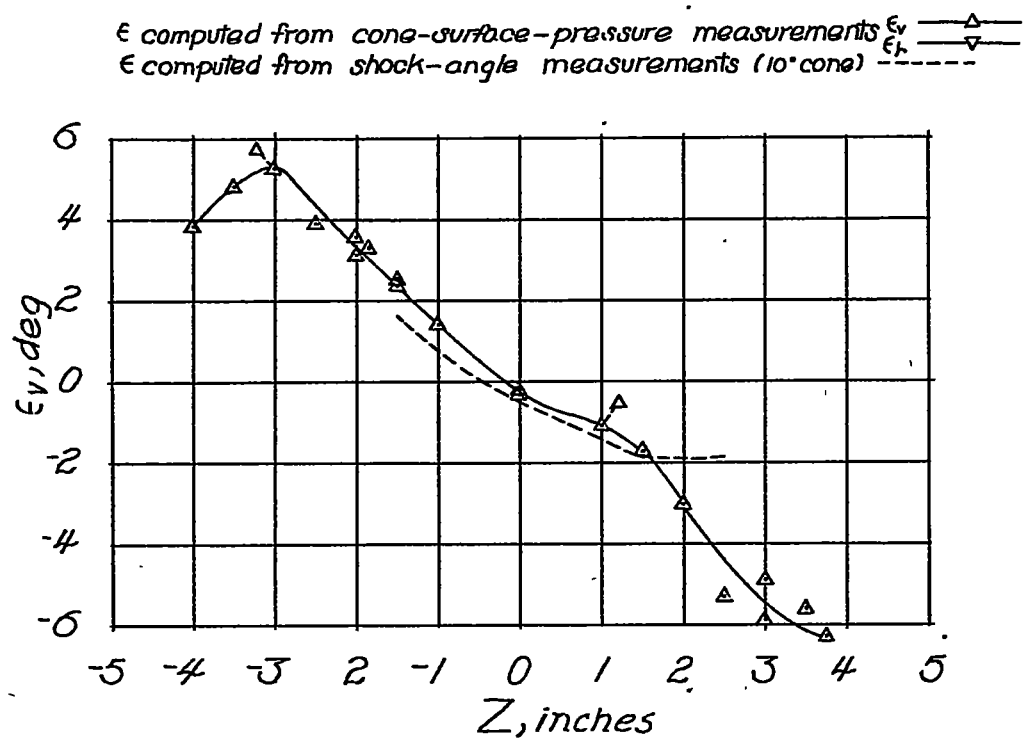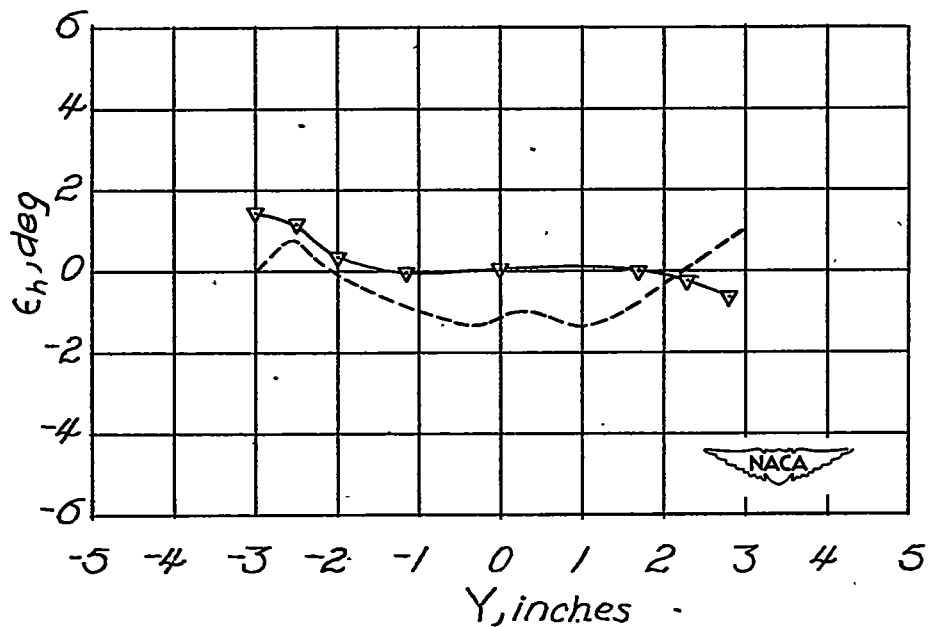

(a) Vertical flow deflection along the vertical center line (Z = 0).

(b) Horizontal flow deflection along the horizontal center line (Y = 0).

Figure 34.— Flow deflections at station 88.5.

ε computed from cone-surface-pressure measurements $\frac{\varepsilon_v}{\varepsilon_h}$ —△—
ε computed from shock-angle measurements (½ cone) ———
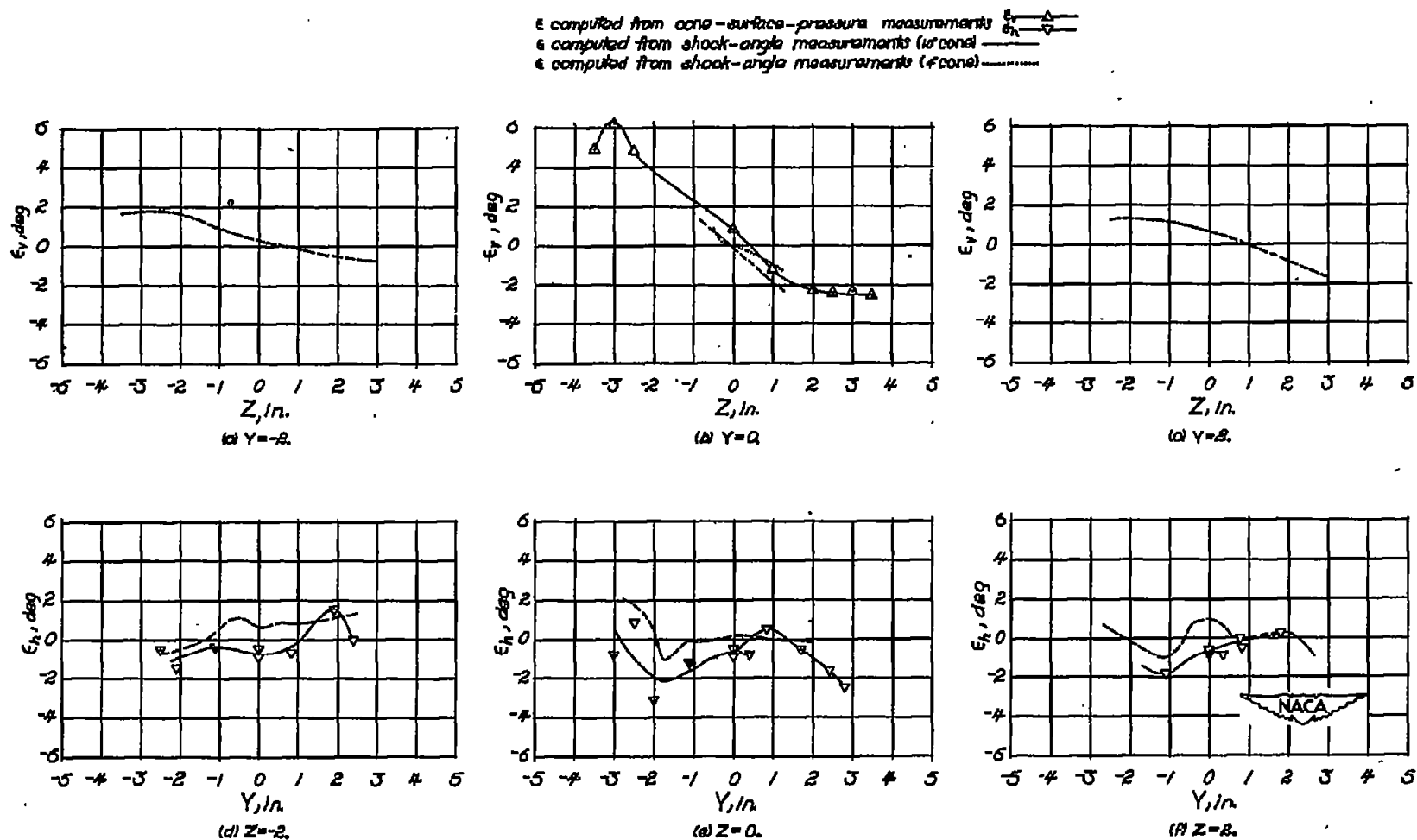ε computed from shock-angle measurements (f cone) ———·——

Figure 35.— Flow deflections at station 90.5.